WILEY

Cladistics

Cladistics (2023) 1–24

10.1111/cla.12538

Systematics and biogeography of the Old World fern genus *Antrophyum*

Cheng-Wei Chen*[a,b,c], Stuart Lindsay[d], Joel Nitta[e], Germinal Rouhan[f], Michael Sundue[g], Leon R. Perrie[h], Yao-Moan Huang[i], Wen-Liang Chiou[i] and Kuo-Fang Chung*[b]

[a]*Biodiversity Program, Taiwan International Graduate Program, Academia Sinica, National Taiwan Normal University, Taipei, 115201, Taiwan;* [b]*Biodiversity Research Center, Academia Sinica, Taipei, 115201, Taiwan;* [c]*Department of Life Science, National Taiwan Normal University, Taipei, 106209, Taiwan;* [d]*Native Plant Centre, Horticulture & Community Gardening Division, National Parks Board, 1 Cluny Road, Singapore, 259569, Singapore;* [e]*Department of Biological Sciences, Graduate School of Science, The University of Tokyo, 2-11-16 Yayoi, Bunkyo-ku, Tokyo, 113-0032, Japan;* [f]*Institut de Systématique, Évolution, Biodiversité, Muséum national d'Histoire naturelle, Sorbonne Université, Ecole Pratique des Hautes Etudes, CNRS, Université des Antilles, Paris, 75005, France;* [g]*Department of Plant Biology, University of Vermont, Burlington, VT, 05405, USA;* [h]*Museum of New Zealand Te Papa Tongarewa, Wellington, 6011, New Zealand;* [i]*Taiwan Forestry Research Institute, Taipei, 100060, Taiwan*

Received 19 September 2022; Revised 7 March 2023; Accepted 21 March 2023

Abstract

Antrophyum is one of the largest genera of vittarioid ferns (Pteridaceae) and is most diverse in tropical Asia and the Pacific Islands, but also occurs in temperate Asia, Australia, tropical Africa and the Malagasy region. The only monographic study of *Antrophyum* was published more than a century ago and a modern assessment of its diversity is lacking. Here, we reconstructed a comprehensively sampled and robustly supported phylogeny for the genus based on four chloroplast markers using Bayesian inference, maximum likelihood and maximum parsimony analyses. We then explored the evolution of the genus from the perspectives of morphology, systematics and historical biogeography. We investigated nine critical morphological characters using a morphometric approach and reconstructed their evolution on the phylogeny. We describe four new species and provide new insight into species delimitation. We currently recognize 34 species for the genus and provide a key to identify them. The results of biogeographical analysis suggest that the distribution of extant species is largely shaped by both ancient and recent dispersal events.

Introduction

The genus *Antrophyum* Kaulf. was established by Kaulfuss (1824) to accommodate five species previously placed in *Hemionitis* L. but distinguished by having linear sori sunken into laminal grooves. The genus has been widely accepted and expanded by subsequent authors, e.g. Bory de St Vincent (1804), Sprengel (1827), Blume (1828), Hooker and Greville (1828) and Kunze (1848). Fée (1852) published the first (and hitherto, only) monographic study of *Antrophyum*, in which he recognized 24 species from both the New and Old World. More species were added in the mid-ninteenth and early twentieth centuries, e.g. Brackenridge (1854), Hooker (1861) and Christ (1907), and the species number increased to more than 30 (Benedict, 1907). As the number of species increased, several authors started to subdivide the genus using morphological traits and geography (Moore, 1857; Benedict, 1907, 1911; Christensen, 1926). Most of these subdivisions were later recognized at genus level in light of molecular phylogenetic analyses (Crane et al., 1995; Crane, 1997; Ruhfel et al., 2008; Schuettpelz et al., 2016). Nowadays, *Antrophyum* is more narrowly circumscribed as a genus restricted to the Old World belonging to subfamily Vittarioideae of Pteridaceae (PPG I, 2016). The genus is most diverse in tropical Asia and the Pacific Islands but is also found in temperate

*Corresponding author:
E-mail address: wade0504@gmail.com; bochung@gate.sinica.edu.tw

Asia, Australia, tropical Africa and the Malagasy region (Schuettpelz et al., 2016). Morphologically, *Antrophyum* differs from the other members of Vittarioideae by the combination of pluriseriate areolate venation, linear sori along veins, soral paraphyses with specialized apical cells (hereafter referred to as simply paraphyses) and trilete spores (Schuettpelz et al., 2016; Fig. 1).

To date, more than 80 basionyms have been published for *Antrophyum* (in its current circumscription) and this number is more than double the generally agreed estimate of about 40 accepted species (Holttum, 1955; Schuettpelz et al., 2016). As demonstrated by recent studies, e.g. Chen et al. (2013, 2017, 2021) and Park et al. (2020, 2021), cryptic species, species complexes, polyploidization and independent gametophytes (gametophytic phase of a fern species existing independently of its sporophytic phase) are all found in the evolution of *Antrophyum*. The traditional morphological approach alone is not enough to provide clear species delimitation since the above processes are not necessarily accompanied by distinguishable morphological changes. More recent studies have integrated morphology and molecular data to explore the diversity of the genus; however, these have focused either on a specific geographic region (East Asia, Chen et al., 2017) or on supporting the recognition of new species (Chen et al., 2015, 2020, 2021). A global scale study of *Antrophyum* is still lacking; thus the true diversity of the genus remains uncertain.

This study aims to address this gap and improve our understanding of the global diversity of *Antrophyum*. We began by enumerating all published names, protologues and types (specimens/images). Using this list, we sought and examined more than 1000 herbarium specimens to generate a preliminary checklist of all tentatively accepted species and their synonyms. This preliminary checklist served as the null hypothesis in our study and was tested by morphometric and molecular phylogenetic analyses. Further, with our robustly supported phylogeny, we conducted divergence time estimates, biogeographic analysis and ancestral trait reconstruction to explore the historical biogeography and patterns of

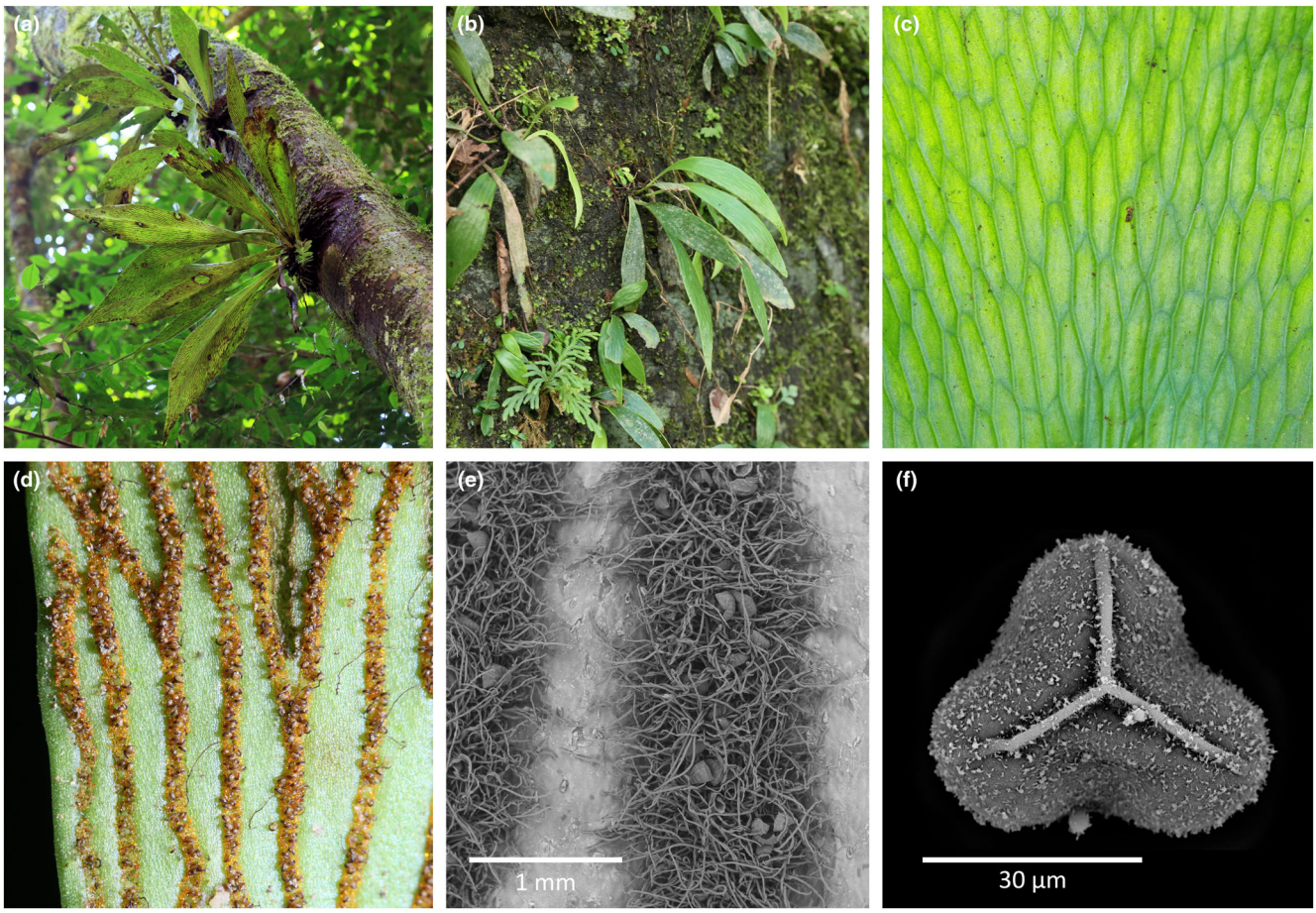

Fig. 1. Habits and key morphological features of *Antrophyum* species. (a) Epiphytic habit of *A. callifolium* Blume (*Chen Wade 5655*); (b) Lithophytic habit of *A. formosanum* (*Chen Wade 5561*); (c) Pluriseriate areolate venation of *A. strictum* (*Chen et al. SITW03597*); (d) Sori of *A. immersum* (*Chen Wade 5670*); (e) Soral paraphyses of *A. hovenkampii* (*Chen Wade 5846*); (f) Tetrahedral spore of *A. plicatum* (*Fraser-Jenkins 33740*).

morphological evolution in the genus. Our study updates the global diversity assessment of *Antrophyum* and will facilitate ecological and evolutionary studies, as well providing a basis for future monographic work.

Materials and methods

Herbarium and field work

We compiled a list of all published names and their corresponding types and protologues from online databases including the International Plant Names Index (www.ipni.org), World Ferns (www.worldplants.de/ferns), Plants of the World Online (www.plantsoftheworldonline.org), JSTOR Global Plants (plants.jstor.org), the Biodiversity Heritage Library (https://www.biodiversitylibrary.org/) and herbarium websites. We also visited or received loans from the following herbaria: A, B, BKF, BM, BO, CAL, CMU, E, GH, IBK, K, KEP, KLU, KUN, KYO, L, M, MICH, MO, NY, P, PE, PSU, RB, S, SAN, SAR, SING, SNP, SZG, TAIF, TNS, U, UC, US and WAG (acronyms follow the Index Herbariorum; sweetgum.nybg.org/science/ih). In total, 1132 specimens were examined. We also did fieldwork in China, Fiji, French Polynesia, Indonesia, Japan, Malaysia, New Caledonia, Singapore, the Philippines, the Solomon Islands, Taiwan and Vietnam to gather additional morphological and ecological data, especially for species that are poorly represented in herbaria or that are inadequately labelled in terms of habit and habitat information. Based on our herbarium and fieldwork, we selected 185 and 122 representative specimens for morphological and molecular phylogenetic analyses, respectively. This sampling covered all species tentatively accepted by us and included multiple specimens for most species to represent their morphological variation and geographical distributions. To make the results from different analyses comparable, we used the same specimens across different analyses whenever possible. Voucher information for all sampled specimens is provided in Table S1.

Morphometric analyses

For each specimen, we measured nine morphological traits found to be informative in previous studies of species delimitation in the genus. Specifically, we measured: the length, width and length/width ratio of the largest fertile frond (CH1–CH3); the length, width and length/width ratio of the apical cells of 30 soral paraphyses (CH4–CH6); the length and width of a representative rhizome scale (CH7 and CH8); and the thickness of 30 cell walls from three rhizome scales (CH9). We used a light microscope (DMR; Leica, Wetzlar, Germany) equipped with a digital camera (EOS 6D; Canon, Tokyo, Japan) and the software ImageJ (Schneider et al., 2012) to photograph and measure the microscopic characters. To determine if the nine traits varied significantly among the species, we conducted one-way ANOVA and subsequent *post-hoc* Tukey highest significant difference pairwise tests. We visualized the results using the R (version 3.4.0; R Core Team, 2017) package "ggplot2" (Wickham, 2009).

Chen et al. (2015) demonstrated considerable variation in the shape of capitate paraphyses (the paraphysis with a swollen apical cell) in *Antrophyum*. To test if the capitate paraphyses can be classified into different shapes, we conducted a geometric morphometric analysis. We included 36 specimens of 20 species with capitate paraphyses in the analysis (Table S1). For each specimen, we digitalized two landmarks and 48 semi-landmarks from images of three representative paraphyses using TPSdig2 (version 2.30; Rohlf, 2015). We placed the two landmarks at the base of each apical cell and the 48 equidistant semi-landmarks along the cell outlines (Fig. 2). We then conducted a generalized Procrustes superimposition using the "gpagen" function in the R package "geomorph" (Adams et al., 2021), which aligns the landmarks (with a least squared approach) and semi-landmarks (with the bending energy algorithm) to remove the information of position, size and orientation, and compare only the shape of the paraphyses. We used the "gm.prcomp" function in the same package to perform a principal component analysis using the Procrustes coordinates resulting from generalized Procrustes superimposition and visualized the result using package "ggplot2" (Wickham, 2009). We tested the statistical significance of the four recognized shapes based on principal component analysis (see Results for details) using the "procD.lm" and "pairwise" functions in the same package.

Molecular phylogenetic analyses

We extracted genomic DNA from fresh, silica-dried or herbarium specimens using the Qiagen DNeasy Plant Mini Kit (Hilden, Germany) following the manufacturer's protocol. We amplified the DNA sequences of four chloroplast regions (*chlL*, *matK*, *ndhF* and *trnL-F*) by PCR as described in Chen et al. (2017) using the primers listed in Table 1. These regions were selected in order to integrate the results with previous studies (Chen et al., 2015, 2017, 2020). In cases where the outermost primers failed in amplifications owing to poor DNA quality (mostly from herbarium specimens), internal primers were used to amplify shorter sequences. A total of 250 sequences were newly published in this study and were deposited in GenBank (Table S1).

DNA sequences were manually assembled and edited using BioEdit (version 7.0.5.3; Hall, 1999) to resolve ambiguous sites. Sequences

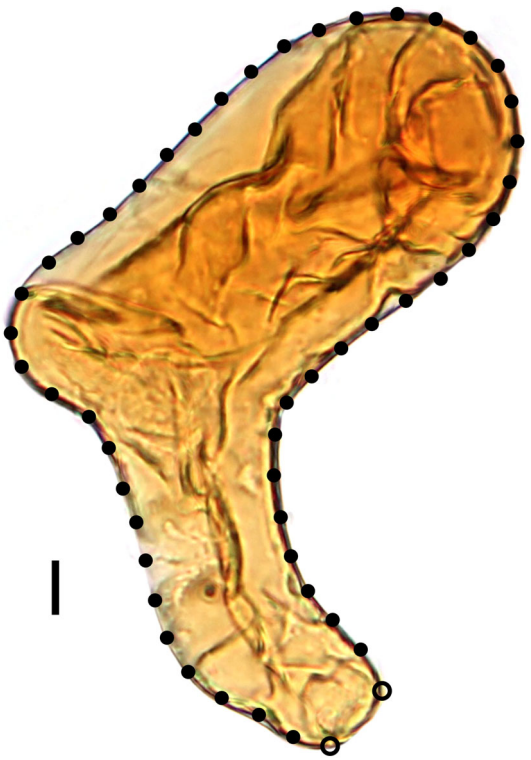

Fig. 2. A representative apical cell of paraphysis (*Antrophyum austroqueenslandicum*) showing the position of the two landmarks (open circles) and 48 equidistant semi-landmarks (closed circles) used in morphometric analysis. Bar = 10 μm.

Table 1
Primers used in amplification and sequencing of the four chloroplast loci (F, forward; I, internal; O, outer; R, reverse)

Locus	Primer	Direction	Location	Sequence (5′–3′)	Reference
chlL	chlN F1	F	O	CCTTCCAAATCCATCTTTATTATCTCTG	Chen et al. (2017)
chlL	trnN R2	R	O	AACCTACGACCAATCGGTTAAC	Chen et al. (2017)
chlL	Ant chlL F	F	I	GGGGGAAGATGCAGGATAG	This study
chlL	Ant chlL R	F	I	CAAAAAGTATGGTAATTACCAGTTTCAC	This study
matK	Vt matK 1610F	F	O	GCARTCAARCGTTTAATTRGTA	Chen et al. (2013)
matK	Vt matK rRFQ	R	O	TTATTACTGAATTTGGRATCT	Chen et al. (2013)
matK	Ant matK 1428F	F	I	AAATCTGTTRCGGGACAGATAAGC	This study
matK	Ant matK 1950R	R	I	CTTGATAAATGCGGAAATGAAACATC	This study
ndhF	Vt ndhF fAYS	F	O	GCTTATTCTACHATGTCTCAGYTRGGATATATGG	Kuo et al. (2017)
ndhF	Vt trnN 2210R	R	O	TCGTGARACGAAAATAGCAGTTTATGG	Kuo et al. (2017)
ndhF	Ant ndhF F1	F	I	TCAGCTGGGATATATGGTTTTATCG	This study
ndhF	Ant ndhF R1	R	I	ATTAAAGAATTGAAAGGGAAACTTAAATC	This study
trnL-F	FernL 1Ir1	F		GGYAATCCTGAGCCAAATC	Li et al. (2010)
trnL-F	F	R		ATTTGAACTGGTGACACGAG	Taberlet et al. (1991)

from each plastid locus were aligned with AliView (version 1.17.1; Larsson, 2014) with MUSCLE (version 3.8; Edgar, 2004) as the default alignment program. Five alignments (four single-locus and one concatenated) were analysed using a maximum likelihood (ML) approach, as implemented in RAxML (version 8.0.3; Stamatakis, 2014). We conducted the analyses under the GTRGAMMA model of sequence evolution and with the optimal partitioning derived from PartitionFinder2 (version 2.2.1; Lanfear et al., 2017), and with 1000 rapid bootstraps (BS) and a subsequent thorough ML search. We manually inspected the topologies generated from five alignments for any well-supported incongruence.

We analysed the concatenated alignment using Bayesian inference (BI) and maximum parsimony (MP). We conducted the BI analyses in MrBayes (version 3.2.6; Ronquist and Huelsenbeck, 2003) with the same optimal partitioning scheme. We computed the Markov chain Monte Carlo (MCMC) in four independent runs of 20 million generations, each run with four chains and sampled every 5000 generations. We checked the convergence of MCMC chains and adequate sampling using Tracer (version 1.7.1; Rambaut et al., 2018). We discarded the first 1 million trees as burn-in and effective sample sizes were higher than 200 for all parameters.

We conducted the MP analyses in PAUP* 4.0a (Swofford, 2002) with all characters treated as unordered and equally weighted. We searched the parsimony trees using the heuristic method with tree bisection–reconnection branch swapping and 500 random-addition-sequence replicates, saving up to 100 trees per replicate. A strict consensus tree was summarized from all the most parsimonious trees found. Bootstrap values were determined with 500 bootstrap pseudoreplicates, each consisting of a heuristic search with a maximum of 100 trees.

Divergence time estimation

We used BEAST (version 2.2.2; Bouckaert et al., 2019) to estimate the divergence time under a Bayesian framework. The analysis was based on a reduced alignment modified from the concatenated alignment used in phylogenetic analysis. Specifically, this reduced alignment included only one specimen for each *Antrophyum* taxon. We also included two and 16 specimens of Dennstaedtiaceae and Pteridaceae, respectively, as the outgroup. We performed 10^8 MCMC chains that sampled every 1000 generations, using a GTR + I + Gamma nucleotide substitution model, an uncorrelated lognormal relaxed clock model and a Yule process tree prior. Because no fossil record of the genus is known, we used two secondary calibration points (the common ancestor of pteroids and vittarioids) derived from Schuettpelz and Pryer (2009) for age constraints under normal distributions. The mean ages for pteroids and vittarioids were set to 110.8 and 45.7 Mya, respectively, and their sigma values were set to 0.5. We used the same methods to confirm the convergence and sampling size as for the phylogenetic analysis.

Historical biogeographic analysis

We used the chronogram resulting from BEAST as the input file for historical biogeographic analysis. We determined geographic distributions for species based upon our own collections that we personally identified in order to avoid problems caused by potential misidentifications. Following the geographical scheme of Brummitt (2001), we recognized six areas: (A) Africa, (B) Asia (Asia-temperate + Indian subcontinent + Indo-China), (C) Malesia, (D) Papuasia, (E) Pacific and (F) Australasia. We chose these areas to best represent the current global distribution of the genus and to detect past major biogeographical shifts within the genus.

We used the R package "BioGeoBEARS" (Matzke, 2013) to perform a likelihood ancestral range estimation using three models: (i) DEC (dispersal extinction cladogenesis, Ree and Smith, 2008), (ii) DIVALIKE (a likelihood-based implementation of dispersal vicariance analysis, Ronquist, 1997); and (iii) BAYAREALIKE (a likelihood implementation of BayArea, Landis et al., 2013). We also tested models with and without founder-event speciation, which is incorporated with the "*j*" parameter in the package. We further evaluated the models under a constrained analysis that considered the dispersal rate differences among the six areas. Specifically, we set a dispersal probability matrix based on the connectivity among the bioregions (1 = high dispersal rate within an area, 0.5 = medium dispersal rate between connected areas and 0.05 = low dispersal rate between disconnected areas, Table 2). In total, we tested 12 models (Table 3) and selected the best-fit model based on the Akaike information criterion (AIC; Burnham and Anderson, 1998) since not all of the models are nested.

We used biogeographical stochastic mapping (BSM) to estimate the frequency of dispersal and vicariance events based on the best-fit model (Dupin et al., 2017). We simulated biogeographic events in *Antrophyum* using 1000 replicates and summarized the mean and standard deviation (SD) of the frequency of events across replicates. When analysing temporal trends in the frequency of biogeographic events, we standardized by total branch length in bins of 2 Myr each, since the number of events scales with branch length (or nodes,

Table 2
Dispersal rates matrix among the six biogeographic areas in our historical biogeography analysis

	A	B	C	D	E	F
A	1	0.5	0.5	0.05	0.05	0.05
B	0.5	1	0.5	0.05	0.5	0.05
C	0.5	0.5	1	0.5	0.5	0.5
D	0.05	0.05	0.5	1	0.5	0.5
E	0.05	0.5	0.5	0.5	1	0.5
F	0.05	0.05	0.5	0.5	0.5	1

A, Africa; B, Asia; C, Malesia; D, Papuasia; E, Australasia; F, Pacific.

Dispersal rates: 1 = within an area; 0.5 = between connected areas; 0.05 = between separated areas.

in the case of cladogenic events) and the total number of branches/nodes increases towards the present (Silvestro et al., 2018). All codes for biogeographical analyses are available at https://github.com/joelnitta/antrophyum_ow.

Morphological character state reconstruction

We used the chronogram resulting from BEAST as the input file for ancestral character reconstruction. For each species, we calculated the averaged value from multiple specimens and log transformed the dataset for standardization. We carried out the maximum likelihood-based reconstructions using the "fastAnc" and the "contMap" functions of the R package "phytools" (Revell, 2012). We estimated the phylogenetic signal of the nine traits using Pagel's λ (Pagel, 1999) and Blomberg's *K* (Blomberg et al., 2003) methods, as implemented in the "phylosig" function of the "phytools" package.

Results

Phylogenetic analyses

Statistics of the five alignments and the phylogenies derived from them are shown in Table 4. Although a precise comparison of the four single-locus alignments and their derived phylogenies was difficult because the number of specimens included in each alignment was different, *matK* and *ndhF* appeared to outperform *chlL* and *trnL-F* because they had a higher percentage of strongly supported nodes (BS ≥80%). Three main clades (Fig. 3, clades A–C) were recovered in all single-locus phylogenies (Figs S1–S4). While several incongruences were found among the four single-locus phylogenies, none of them was highly supported. As a result, the following analyses and discussions are based only on the concatenated alignment since it provided the highest resolution.

The tree topologies generated from the BI, ML and MP analyses were mainly identical, except for poorly supported nodes (Figs S5–S7). The ML phylogram reconstructed from the concatenated alignment is shown in Fig. 3. We found *Antrophyum* to be strongly supported (BS 100%, posterior probabilities (PP) 1.0) as monophyletic, with the oldest divergence separating a New Caledonian endemic species, *A. novae-caledoniae* Hieron., from the remainder (Fig. 3, clade A). The second divergence resulted in two clades

Table 3
Results of the BioGeoBEARS analysis

Model	Geographical constrain	LnL	No. of parameters	*d*	*e*	*j*	AIC
DEC	Unconstrained	−96.18	2	0.01	0.01	0.00	196.36
DIVALIKE	Unconstrained	−107.11	2	0.02	0.02	0.00	218.22
BAYAREALIKE	Unconstrained	−106.30	2	0.01	0.09	0.00	216.60
DEC + *j*	Unconstrained	−92.16	3	0.01	0.01	0.00	198.31
DIVALIKE + *j*	Unconstrained	−100.90	3	0.01	0.00	0.06	207.79
BAYAREALIKE + *j*	Unconstrained	−101.84	3	0.01	0.07	0.02	209.68
DEC	Constrained	−92.57	2	0.04	0.01	0.00	189.15
DIVALIKE	Constrained	−104.37	2	0.06	0.01	0.00	212.74
BAYAREALIKE	Constrained	−105.56	2	0.04	0.09	0.00	215.13
DEC + *j*	Constrained	−89.95	3	0.03	0.00	0.08	185.89
DIVALIKE + *j*	Constrained	−98.62	3	0.04	0.00	0.14	203.24
BAYAREALIKE + *j*	Constrained	−105.29	3	0.07	0.06	0.12	216.59

LnL (log-likelihood score), AIC (Akaike information criterion) and model parameters rounded to two decimal digits.

Table 4
Statistics for the ingroup DNA sequence alignments used in this study (BS = maximum likelihood bootstrap support)

Loci	Alignment length (bp)	Variable sites (bp, %)	Missing data (%)	Mean BS (%)	Node with BS ≥80% (%)
chlL	879	226 (25.1)	15.4	50	23.8
matK	1041	548 (52.6)	21.9	76	55
ndhF	1182	386 (32.7)	18.5	71	51.2
trnL-F	971	344 (35.4)	14.8	66	39.3
Concatenated	4073	1201 (29.5)	17.3	78	61.7

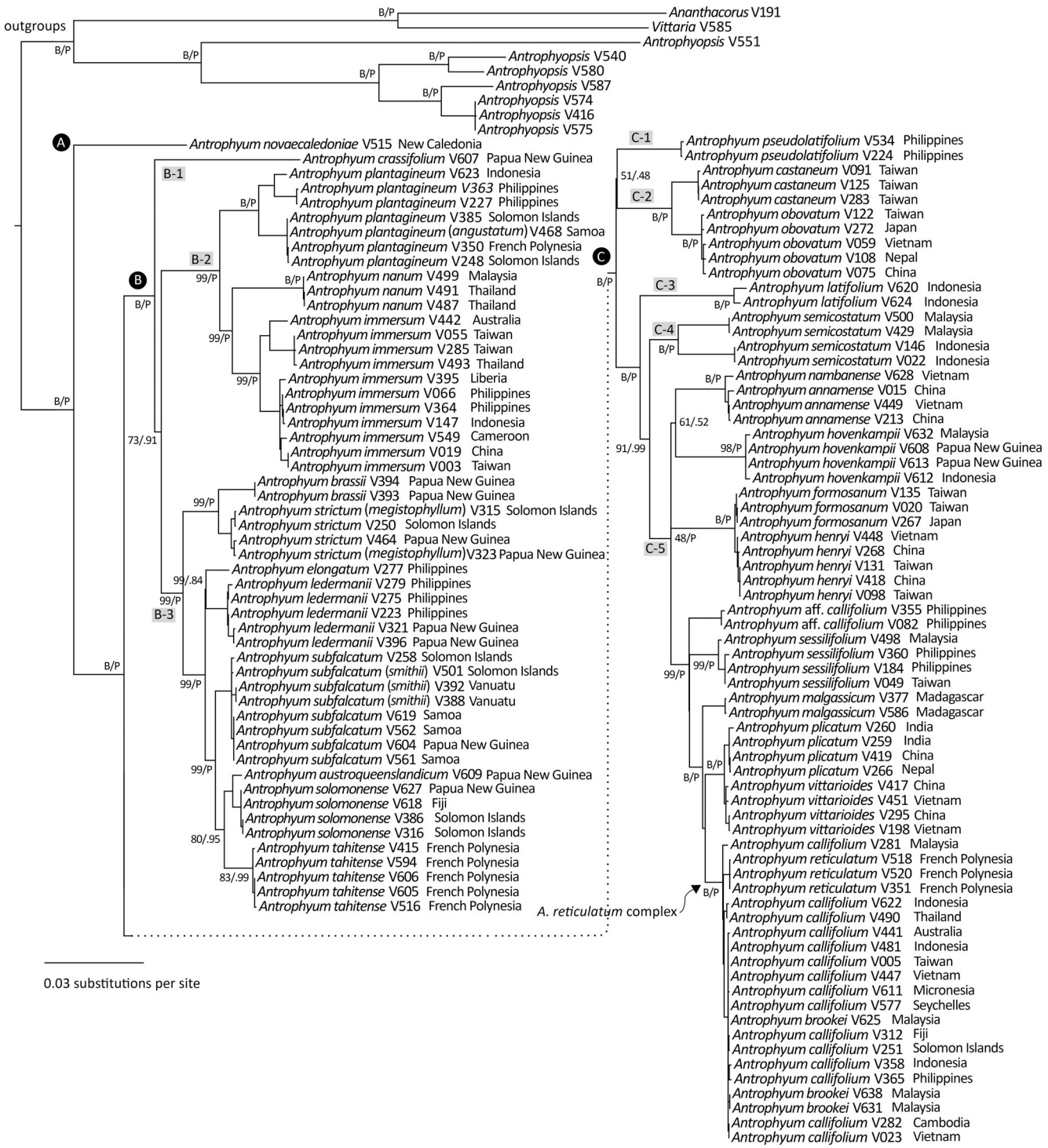

Fig. 3. *Antrophyum* phylogeny resulting from maximum likelihood analysis of a four-gene (*chlL*, *matK*, *ndhF* and *trnL-F*) plastid dataset including 122 ingroup and eight outgroup specimens. Maximum likelihood bootstrap percentages (BS) and Bayesian posterior probabilities (PP) are provided at selected nodes (BS/PP; $B = 100$; $P = 1.00$). The major clades/subclades discussed in the text are indicated. Numbers following species names are DNA voucher numbers (Table S1). The original morphology-based identifications are shown in parentheses (see the Discussion).

(Fig. 3, clades B and C) with a moderate geographic pattern. Clade B consisted of species mostly from Malesia, Australia and the Pacific Islands whereas clade C consisted of species mostly from Asia. We also found a strong morphological pattern between the two clades. Specifically, clade B was composed of species

that only have capitate paraphyses, whereas clade C was composed of species with a disparate assemblage of capitate, taeniform, and filiform paraphyses. To facilitate further discussions, we recognized three and five subclades for clades B (B-1 to B-3) and C (C-1 to C-5), respectively (Fig. 3).

Overall, inter-species relationships were well resolved. Among the 128 resolved nodes, 79 of them received good support (BS > 80%, PP > 0.95). Most of the poorly supported (BS < 80%, PP < 0.95) nodes were found within species, with only five exceptions. Among the 26 species with multiple samples, 24 of them were strongly supported (BS 100%, PP 1.0) as monophyletic. The two exceptions were *A. brookei* Hook. and *A. callifolium* Blume, which were resolved as polyphyletic in our analysis.

Morphometric analyses

The results of measurements are provided in Table S1. Illustrations of representative fronds, paraphyses and rhizome scales of all the species are shown in Figs 4–6, respectively. All the nine measured traits varied among species (Figs S8–S16) and their pairwise *P*-values are shown in Tables S2–S4. Generally, we observed larger intra-species variation in the size/shape of fronds and scales, whereas the morphology of paraphyses was more homogenous within a species. The two exceptions were *A. austroqueenslandicum* D.L. Jones and *A. solomonense* C.W.Chen & J.H.Nitta, which have both clavate and boot-shaped paraphyses as described in Chen et al. (2015).

Based on the size (length, width) and length/width ratio of the paraphyses, we recognized three main types of paraphyses, i.e. capitate, filiform and taeniform (Table 5). We further classified the capitate paraphyses into four shapes (i.e. oblong, oblate, clavate and globose) based on the results of geometric morphometric analysis (Fig. 7, Table 6). Among the oblong and globose paraphyses, we also found considerable size variation that enabled us to further classify them as large or small. Combining the results for paraphyses size, shape and the presence of boot-shaped paraphyses, we eventually classified the capitate paraphyses into seven subtypes (Table 7).

Molecular dating and historical biogeography

The chronogram inferred by BEAST with the ancestral range estimated by BioGeoBEARS is summarized in Fig. 8. The tree topology derived from BEAST was identical to that from RAxML. The divergence of *Antrophyum* and its sister genus *Antrophyopsis* (Benedict) Schuettp. was dated back to the middle Oligocene around 30 Mya (95% highest posterior density, HPD = 24.0–36.1 Mya). Within the genus, the first and second divergences dated back to around 20 Mya (95% HPD = 15.3–25.6 Mya) and 16 Mya (95% HPD = 11.8–20.3 Mya).

Among the 12 biogeographic models tested, we determined the constrained DEC + *j* model as the best-fit model because it yielded the lowest AIC value (Table 3). Table 8 shows the most likely ancestral range of each clade, together with divergence-time estimates. The best-fit model suggested that the ancestor of *Antrophyum* was widely distributed in Malesia, Papuasia and the Pacific Islands. Nonetheless, there is high uncertainty in ancestral ranges (Fig. S17). Papuasian and Malesian origins were inferred for Clades B and C, respectively. These clades began to expand into other areas about 10 Mya.

Range expansions were the most frequently observed biogeographic event over all BSM replicates (mean 18.42 ± 1.72 events per replicate; Table 9). The most frequently observed dispersal patterns were between Malesia and Papuasia, from Papuasia to the Pacific, and between Asia and Malesia (Fig. S18a). Vicariance events were most frequent early in the history of *Antrophyum*, and decreased with time towards the present (Fig. S19a). Dispersal events increased in the most recent 10 Myr (Fig. S19d).

Morphological character state reconstruction

The results of ancestral character reconstruction of the nine analysed morphological traits are shown in Fig. 9. A phylogenetic signal test statistically examines if the observed trait distribution along the phylogeny is significantly different from a random distribution. Among the nine traits, three and four traits showed significant phylogenetic signals ($P < 0.05$) in Pagel's λ and Blomberg's K indices, respectively. The traits of soral paraphyses (CH4–CH6) showed higher phylogenetic signals. In contrast, those of fronds (CH1–CH3) and rhizome scales (CH7–CH9) showed lower phylogenetic signals.

Discussion

Origin and historical biogeography of Antrophyum

Our study presents the first comprehensive phylogenetic analysis of *Antrophyum*. Among the 34 species tentatively recognized, only three (*A. kinabaluense* C.W.Chen, *A. marginale* Blume and *A. simulans* Alderw.) are missing in the current analysis and it is unlikely they will affect the main conclusions (see later Discussion). The time-calibrated phylogeny reveals that the common ancestor of *Antrophyum* and its sister group *Antrophyopsis* diverged in the middle Oligocene

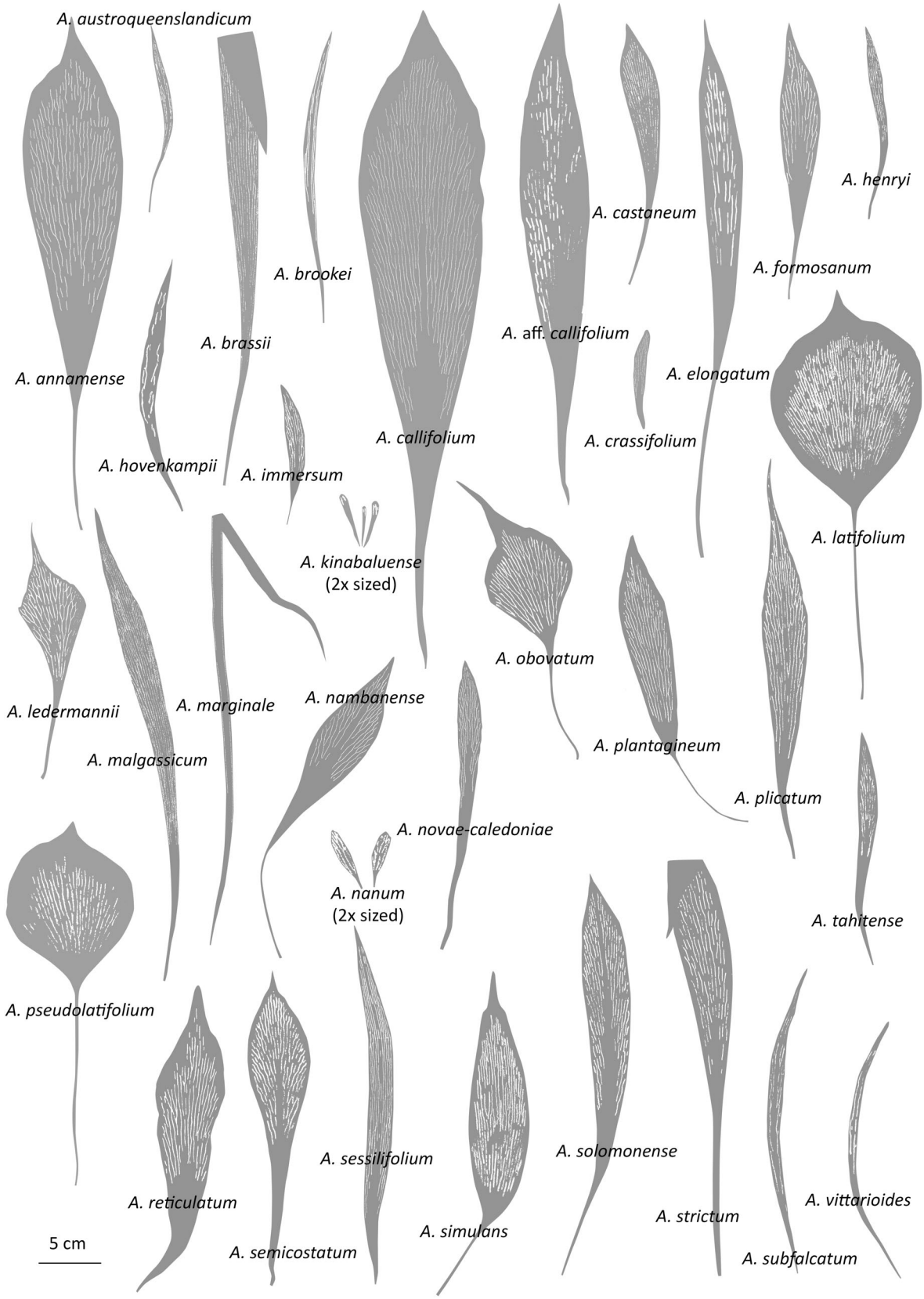

Fig. 4. Frond shapes and soral line distributions of 34 *Antrophyum* species.

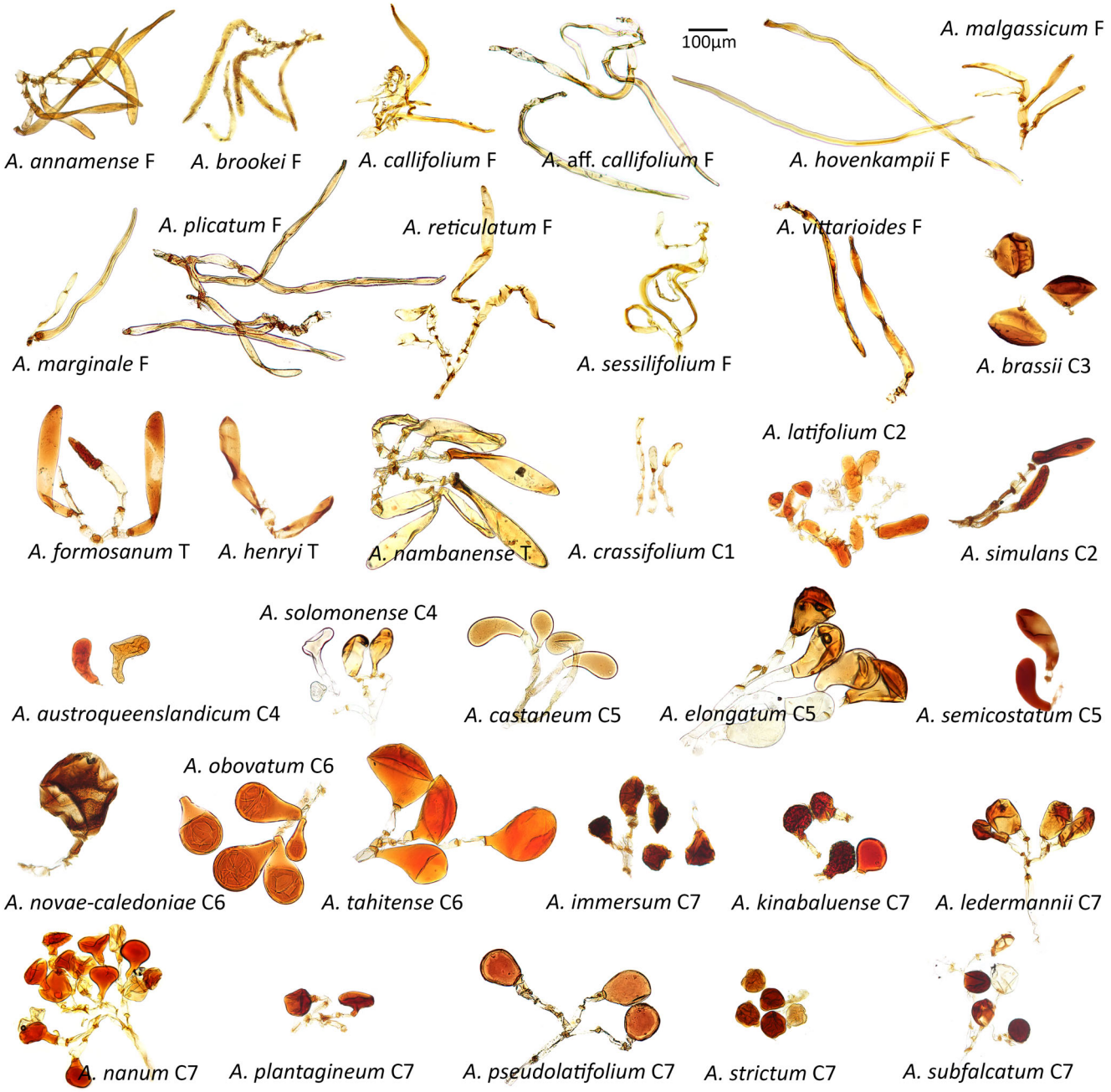

Fig. 5. Apical cells of soral paraphyses of 34 *Antrophyum* species. Paraphyses type is indicated after species name: C, capitate; F, filiform; T, taeniform. Capitate paraphyses are further classified into seven subtypes (C1–C7) as shown in Table 7.

around 30 Mya (95% HPD = 23.9–36.1 Mya). The current allopatric distribution of *Antrophyum* (mainly tropical Asia and Pacific Islands) and *Antrophyopsis* (African endemic) is probably the result of transoceanic dispersal since the two landmasses were already separated at that time. At least one dispersal event was observed in 632 of the 1000 BSM replicates along the branch leading to *Antrophyum*. Dispersal seems to have played an important role in the biogeographic history of *Antrophyum*, with an average of 22.7 dispersal events (range expansions or founder events) per BSM replicate, but only 3.63 vicariance events (Table 9).

Although the estimation of ancestral ranges under the best-fit model (constrained DEC + *j*) suggests that the ancestral range of the crown group of *Antrophyum* was the landmasses of today's Malesia (C), Papuasia (D) and Pacific (E), the low probability of this result

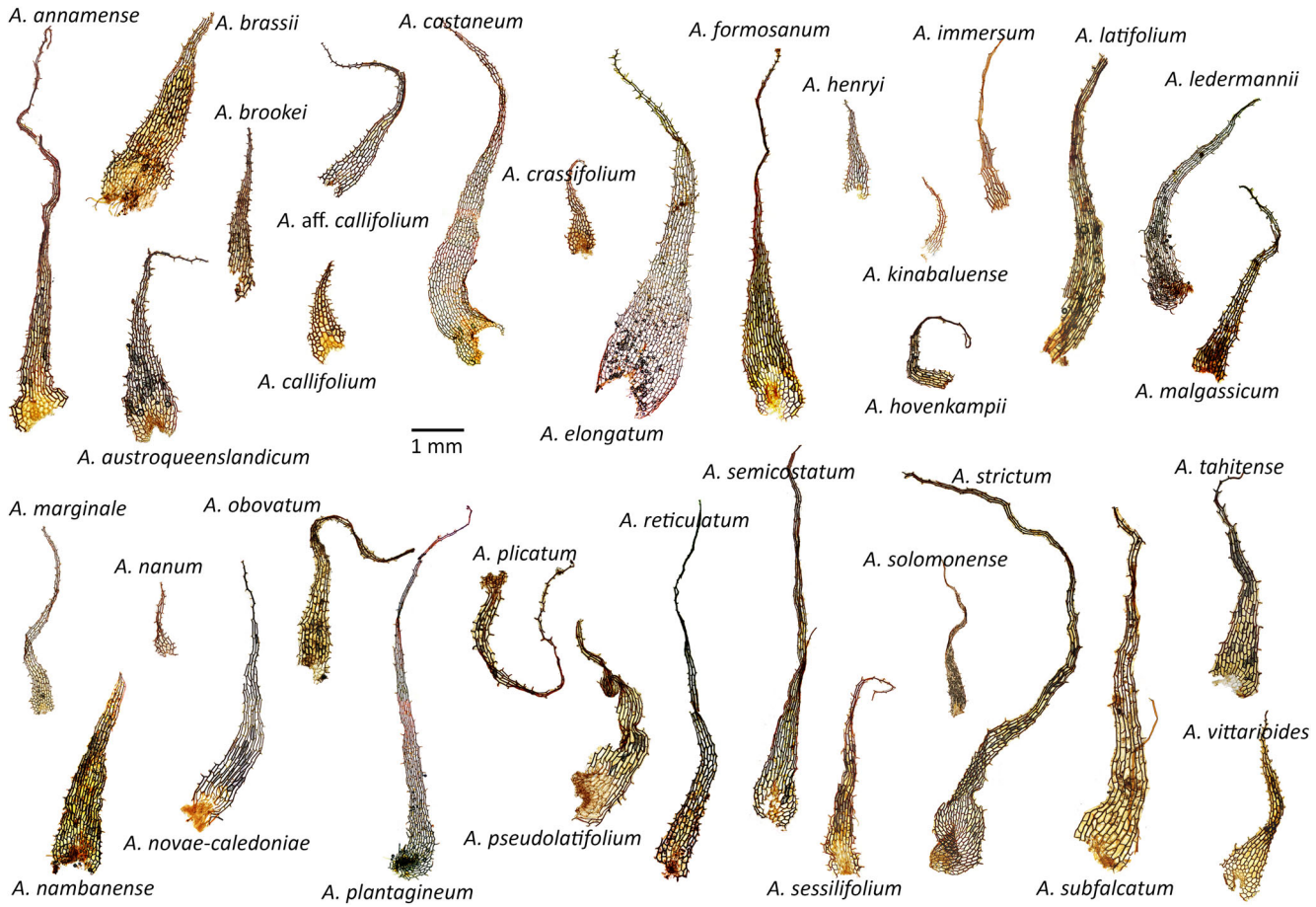

Fig. 6. Rhizome scales of 33 *Antrophyum* species. *Antrophyum simulans* is not included owing to a lack of material.

(15%, Table 8) leaves the ancestral distribution of the genus uncertain. Unexpectedly, the New Caledonian endemic *A. novae-caledoniae* is recovered as sister to all other extant *Antrophyum* species in this analysis. Their divergence was dated to the early Miocene around 20 Mya (95% HPD = 15.3–25.6 Mya). A similar pattern has been observed in several other plant groups (Álvarez-Molina and Cameron, 2009; Vasconcelos et al., 2017) and the most well-known example is the flowering plant *Amborella* Baill., which is endemic to New Caledonia and sister to all other angiosperms (Simmons, 2017). So-called relict lineages seem to be over-represented in New Caledonia, and this has been attributed to the persistence of forest throughout the Neogene that acted as refugia while extinctions happened elsewhere (Pouteau et al., 2015; Condamine et al., 2017; Pillon et al., 2021).

Clades B and C, together, include almost all the extant species of *Antrophyum*, but there is a clear difference in the geographic origins with clade B originating in Papuasia and clade C originating in Malesia (Table 8). Clade B subsequently colonized eastward to the Pacific Islands and westward to Malesia while clade C colonized northward to Asia. The extent to which the contrasting biogeographic histories of clades B and C reflect ecological differences remains to be investigated. Long distance dispersal, in particular range expansions, increased in frequency during the past 10 Mya (Fig. S19b). Although the overall trend was dispersal eastward (from Papuasia or Malesia to the Pacific Islands) or northward (from Malesia to Asia), the analysis also suggests several westward dispersal events in clade B. For example, the B-2 and B-3 clades dispersed from Papuasia to Malesia (means of 0.65 ± 0.86 and 1.05 ± 0.67 such dispersal events per BSM replicate, respectively). Long-distance dispersal that crossed the Indian Ocean (from Malesia to Africa) probably happened at least twice, once in *A. immersum* (Bory ex Willd.) Hook. & Baker and the other in the clade containing *A. sessilifolium* (Cav.) Spreng., *A. malgassicum* C.Chr. and closely related species (means of 0.71 ± 0.46 and 0.52 ± 0.66 such dispersal events per BSM replicate, respectively).

Table 5
Three main types of apical cells of soral paraphyses recognized and their sizes (mean ± standard deviation)

	Capitate (n = 2110)	Taeniform (n = 395)	Filiform (n = 1250)	P
Length (μm)	106.4 ± 42.4	303.3 ± 108.3	496.3 ± 210.8	<0.001*
Width (μm)	75.6 ± 32.2	44.2 ± 8.7	23.6 ± 5.4	<0.001*
Length/width	1.6 ± 0.8	7.0 ± 2.6	22.2 ± 10.9	<0.001*

*Significances (P < 0.05).

Taxonomic value and evolution of morphological traits

This study is the most comprehensive morphological investigation of the genus *Antrophyum* to date and this enables us to evaluate the taxonomic value of each trait. Concordant with many previous studies (Chen et al., 2015, 2021), we find that the apical cells of soral paraphyses are arguably the most useful taxonomic trait. To our knowledge, Blume (1828) was the first to describe the morphology of paraphyses when publishing new species of *Antrophyum*. Specifically, he described *A. callifolium*, *A. reticulatum* (G.Forst.) Kaulf., and *A. marginale* as having "hairy sori" (soris villosis), and *A. semicostatum* Blume as having "swollen sori" (sorisque turgidioribus). Fée (1852) described the paraphyses of every species in his monograph of the genus. Since then, paraphyses have become one of the commonly used traits for species delimitation (Holttum, 1955; Zhang, 1998). Conventionally, most authors have recognized three types of paraphyses, i.e. filiform, taeniform and capitate, and we do too (Table 5). Based on the results of our character state

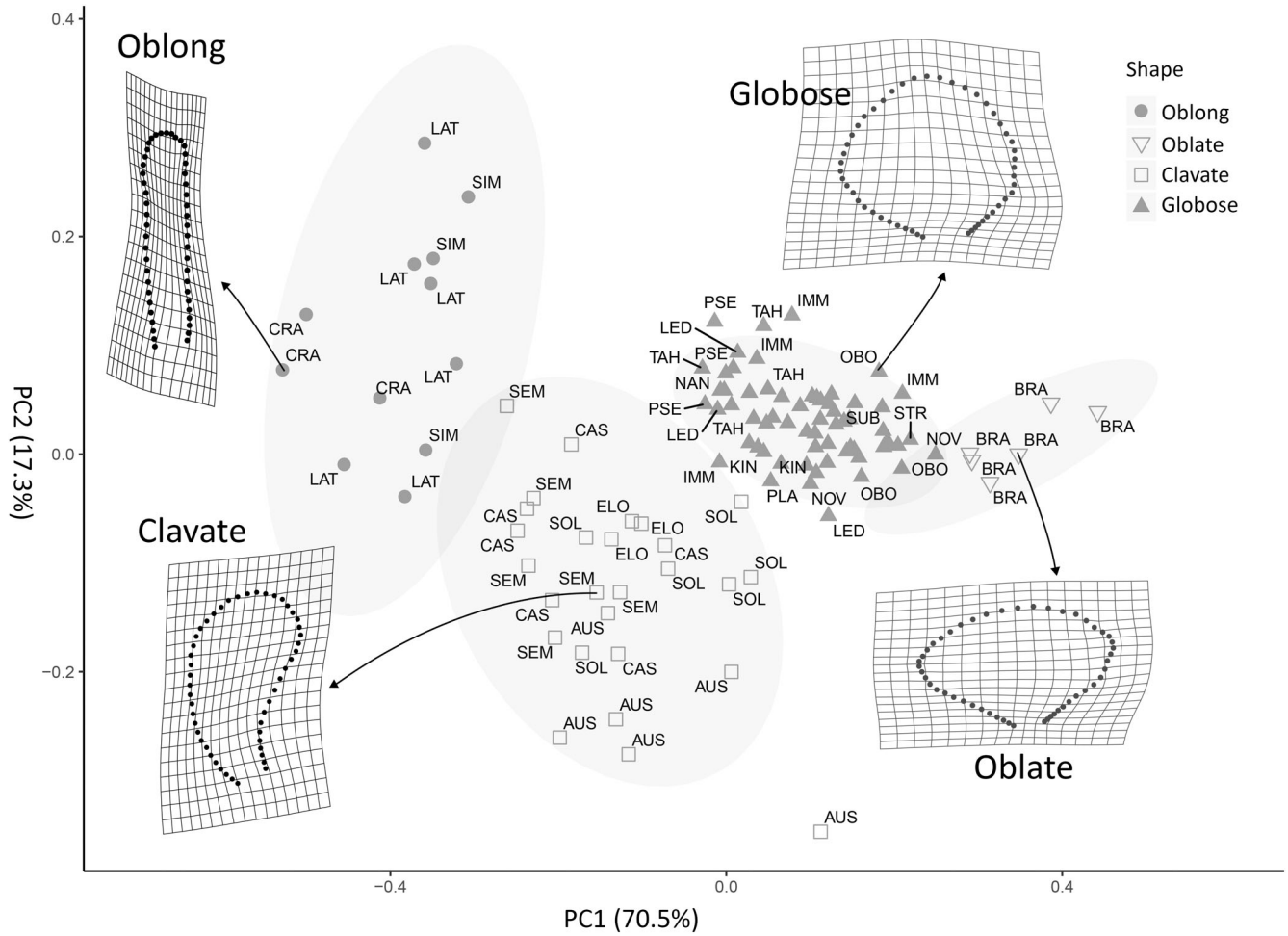

Fig. 7. Principal component analyses comparing four apical cells shapes (clavate, globose, oblate and oblong) of 20 *Antrophyum* species with capitate paraphyses. Each point represents a paraphysis and is labelled with the species names (abbreviated by the first three letters of their epithets). Out of 108 paraphyses included in the analysis, 53 are not labelled for better visualization (they are highly overlapped). For each shape, a represented specimen is visualized.

Table 6
Results of the Procrustes ANOVA which tested the differences between the four shapes of capitate paraphyses and 20 taxa with capitate paraphyses

	d.f.	SS	MS	R^2	F	Z	Pr (>F)
Type	3	4.2652	1.42173	0.71481	86.89	8.4148	<0.001
Taxa	19	4.8667	0.256140	0.81561	20.487	9.6957	<0.001

d.f., degrees of freedom; SS, sum of squares; MS, mean square.

Table 7
Seven subtypes of capitate paraphyses classified according to the shape and size of their apical cells

Type	Shape	Size (length × width μm)	Species	Clade
1	Oblong	42–82 × 15–39, S	*Antrophyum crassifolium*	B-1
2	Oblong	85–209 × 24–66, L	*A. latifolium*	C-3
2	Oblong	97–176 × 27–64, L	*A. simulans*	NA
3	Oblate	57–114 × 70–170	*A. brassii*	B-3
4	Clavate*	85–192 × 26–89	*A. austroqueenslandicum*	B-3
4	Clavate*	44–159 × 39–122	*A. solomonense*	B-3
5	Clavate	74–215 × 37–92	*A. castaneum*	C-2
5	Clavate	92–167 × 61–103	*A. elongatum*	B-3
5	Clavate	51–259 × 30–78	*A. semicostatum*	C-4
6	Globose	160–299 × 148–271, L	*A. novae-caledoniae*	A
6	Globose	89–257 × 65–187, L	*A. obovatum*	C-2
6	Globose	77–195 × 60–181, L	*A. tahitense*	B-3
7	Globose	47–155 × 38–118, S	*A. immersum*	B-2
7	Globose	73–112 × 66–110, S	*A. kinabaluense*	NA
7	Globose	61–176 × 51–99, S	*A. ledermannii*	B-3
7	Globose	57–122 × 50–104, S	*A. nanum*	B-2
7	Globose	37–109 × 26–118, S	*A. plantagineum*	B-2
7	Globose	52–159 × 43–108, S	*A. pseudolatifolium*	C-1
7	Globose	46–93 × 44–96, S	*A. strictum*	B-3
7	Globose	48–108 × 45–98, S	*A. subfalcatum*	B-3

The oblong and globose paraphyses are further classified into small (S) and large (L) ones.

*The two species with boot-shaped paraphyses. The phylogenetic placement of each species is shown except for *A. simulans* and *A. kinabaluense*.

reconstruction, we found that these three paraphyses types show a constant phylogenetic signal. Chen et al. (2015) illustrated the shape variation of capitate paraphyses. In this study, we extended the exploration of the taxonomic value of capitate paraphyses using shape analysis. We found significant shape and size differences among the species and eventually classified the capitate paraphyses into seven subtypes (Table 7).

Other traits that have been used or suggested to be of potential use for species delimitation in vittarioid ferns but not analysed in this study include the distribution of sori, paraphyses branched/unbranched, stipes present/absent, the shape of the stipe in cross section, superficial or immersed soral lines, and silica bodies within the laminae. Based on the previous studies and our observations, all the above traits can be useful in identifying specific species of *Antrophyum* or distinguishing similar species pairs. The difficulty in quantifying these traits is the main reason we did not include them in our analyses, but their taxonomic value does deserve further exploration. For example, the stipes of *A. latifolium* Blume and *A. obovatum* Baker are always very distinct and can be used to distinguish these two species from the others. However, for majority of the species, their laminae gradually reduce to the base, making it difficult to provide a clear definition for stipes. Chen et al. (2019) found silica bodies useful for distinguishing two morphologically similar *Haplopteris* C.Presl species. Our preliminary observations show considerable variability in the outline of silica bodies among the *Antrophyum* species. A wider and deeper sampling is still needed to explore the variation and taxonomic value of silica bodies.

Antrophyum reticulatum and *A. semicostatum* complexes

Antrophyum callifolium and *A. reticulatum* are the two names most widely applied to plants with filiform paraphyses (e.g. Asia: India, Fraser-Jenkins et al., 2017; Taiwan, TPG, 2019; Malesia: Malaysia, Lindsay and Middleton, 2020; New Guinea, Cámara-Leret et al., 2020; Pacific Islands: Solomon Islands,

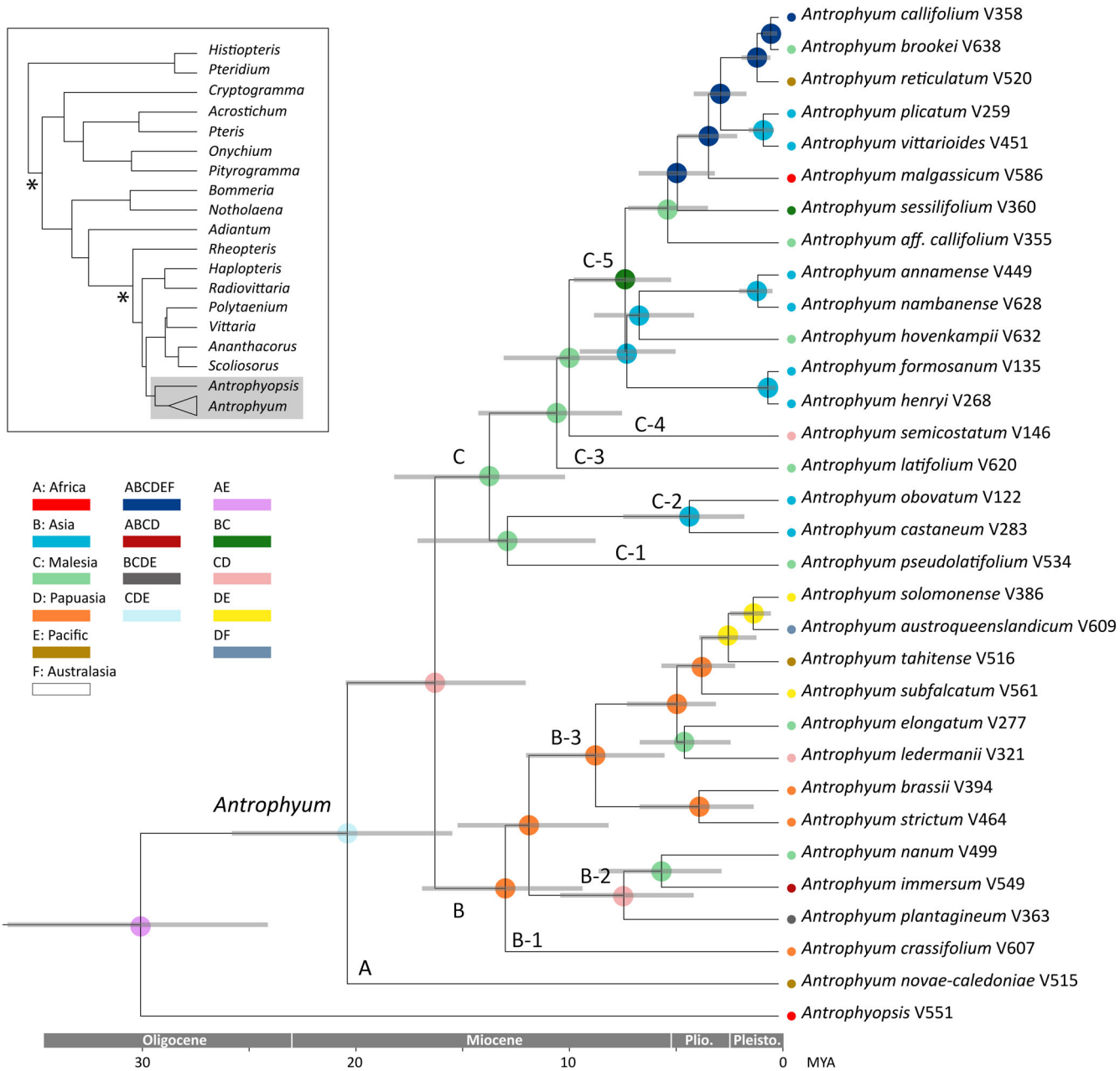

Fig. 8. Time-calibrated trees showing generic-level relationship of Pteridaceae (inset) and the species-level relationship of *Antrophyum* based on four chloroplast regions using BEAST. Asterisks (*) indicate the two secondary calibrations points. Ancestral range estimation for *Antrophyum* was performed with BioGeoBEARS under the dispersal–extinction–cladogenesis model (DEC) and constrained dispersal rates. The distribution of each species is mapped to the right of the chronogram. The single-most-probable state (geographical range) is shown at each node. Grey bars on nodes indicate the 95% highest probability density interval of the age.

Chen et al., 2022; Vanuatu, Plunkett et al., 2022). *Antrophyum reticulatum* was described from Society Islands, under the genus *Hemionitis* by Forster (1786) and later transferred to *Antrophyum* by Kaulfuss (1824). Four years later, Blume (1828) described *A. callifolium* from Java, Indonesia, distinguishing it from *A. reticulatum* by its thicker and larger fronds. However, specimens with intermediate morphology are abundant in herbaria and laminae texture and size are inadequate characters by which to separate them. So far, the morphological delimitation between these two species has not been well investigated (Holttum, 1955), and their names have often been misapplied in the past (see arguments of Fraser-Jenkins et al., 2017). Furthermore, their relationship with several other congeneric species with filiform paraphyses is far from clear, and

Table 8
Bayesian posterior divergence-time estimates (median and 95% highest posterior density, HPD) for the main clades of *Antrophyum*, along with the most probable ancestral ranges (C, Malesia; D, Papuasia; E, Pacific)

Clade	Stem group age in Myr (95% HPD)	Crown group age in Myr (95% HPD)	Most probable ancestral ranges (%)
Antrophyum	29.9 (23.9–36.1)	20.2 (15.3–25.6)	CDE (15)
B + C	20.2 (15.3–25.6)	16.1 (11.8–20.3)	CD (17)
B	16.1 (11.8–20.3)	12.8 (9.1–16.7)	D (62)
C	16.1 (11.8–20.3)	13.5 (10.0–18.0)	C (42)

Table 9
Frequency of biogeographic events observed over 1000 biogeographical stochastic mapping (BSM) replicates using best-scoring model (constrained DEC + *j*)

Mode	Event	Mean	SD
Within-area speciation	Subset (*s*)	11.25	3.09
Within-area speciation	Sympatry (*y*)	11.84	2.08
Dispersal	Founder (*j*)	4.28	1.62
Dispersal	Range expansion (*d*)	18.42	1.72
Vicariance	Vicariance (*v*)	3.63	1.47

Letters in parentheses indicate names of parameters in the BioGeoBEARS model. No extinction events were observed.

many names have been synonymized under each of them (Christensen, 1905–1906; Zhang, 1998; Fraser-Jenkins et al., 2017). Here, we refer to this group of species as the *A. reticulatum* complex. To our knowledge, this complex includes at least 14 published names as listed in Table S5 and four of them (i.e. *A. brookei*, *A. marginale*, *A. callifolium* and *A. reticulatum*) are tentatively accepted as distinct species in this study.

We confine the use of the name *A. reticulatum* to only those specimens collected in French Polynesia, its type locality. Two additional names, *A. durvillaei* Bory and *A. grevillei* Balf. ex Grev., have been published for specimens from the area; morphologically they differ from other members of the complex by having significantly thicker rhizome scale cell walls (Fig. S16). The types of *A. reticulatum* and *A. durvillaei* are very similar in terms of morphology and are thus likely to be conspecific, but together they can be distinguished from the type of *A. grevillei* by frond shape (falcate vs. linear). We included three specimens of typical *A. reticulatum* (i.e. falcate fronds) in the phylogenetic analyses and they were genetically almost identical and formed a clade that was paraphyletic with respect to *A. callifolium* and *A. brookei*. Although we think *A. grevillei* should be conspecific with *A. reticulatum* because of the specimens with intermediate frond shape present in herbaria, future studies should include a specimen resembling the type of *A. grevillei* (i.e. with linear fronds) to test if *A. grevillei* is a distinct species.

Antrophyum brookei and *A. marginale* are unique in the *Antrophyum reticulatum* complex in having narrowly linear fronds (Fig. 4). These two species can be distinguished from each other by the distribution of their sori. Specifically, *A. marginale* usually has two long uninterrupted lines of sori (only a little shorter than the frond), one on each half of the lamina close to the margin. In contrast, fully developed fronds of *A. brookei* usually have two to six shorter sori lines (no more than half the length of the frond) that are not confined to the margin. We included three specimens of *A. brookei* in the phylogenetic analyses and, surprisingly, they turned out to be polyphyletic and mixed with *A. callifolium*. However, both the specimen records and our field observations show that *A. brookei* is a rheophyte growing by rivers or streams (sometimes only a few centimetres above water), whereas *A. callifolium* is an epiphyte or lithophyte. This suggests that *A. brookei* might be a recently diverged lineage from *A. callifolium* that adapted to rheophytic habit. Possibly, these two species have not yet reached reciprocal monophyly because of their short divergence time (Fig. 8), but *A. brookei* probably represents an evolutionary significant unit because of its morphological and ecological distinctness.

As circumscribed in this study, *A. callifolium* is the most widely distributed species of the genus. It occurs in Pacific Islands, Australia and Asia and is one of only two species in the genus that has successfully crossed the Indian Ocean and colonized Africa (the other is *A. immersum*, Fig. 8). We included 15 specimens covering its global distribution in the phylogenetic analysis and found that the genetic variation of this widely distributed species is surprisingly small (Kimura's two-parameter (K2P) distance 0.0017) and not larger than some narrowly distributed species such as *A. annamense* Tardieu & C.Chr. (K2P distance 0.0019, only found in Hainan Island and Northern and Central Vietnam) and *A. vittarioides* Baker (K2P distance 0.0015, only found in Southwestern China and Northern Indochina). This suggests that either continuous gene flows occur among the populations of *A. callifolium* and all the populations can be considered to be panmictic or *A. callifolium* has experienced a very recent and rapid expansion.

In addition to the four tentatively accepted species discussed above (i.e. *A. brookei*, *A. callifolium*, *A. marginale* and *A. reticulatum*), special attention should be paid to *Antrophyum rigidum* (Cav.) comb. ined. (basionym *Hemionitis rigida* Cav.), which is one of the earliest species epithets referable to the genus. It was described from Luzon in the Philippines by Cavanilles (1802), but was subsequently neglected by later authors and has not yet been formally

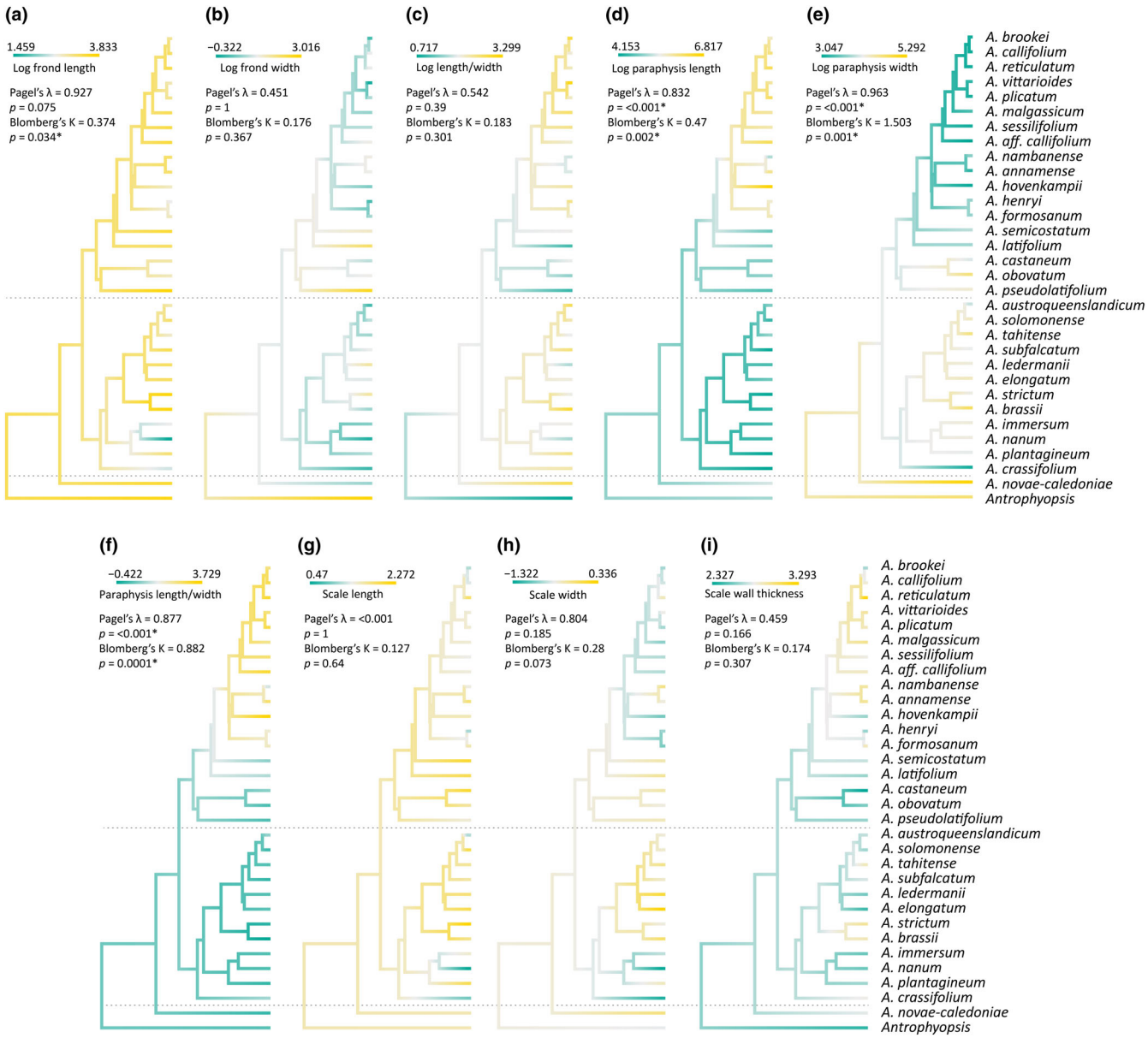

Fig. 9. Ancestral character reconstruction of the nine traits and their phylogenetic signal estimating using Pagel's λ and Blomberg's *K*. Asterisks indicate significances ($P < 0.05$). (a) frond length, (b) frond width, (c) frond length/width ratio, (d) paraphyses length, (e) paraphyses width, (f) paraphyses length/width ratio, (g) scale length, (h) scale width and (i) scale cell wall thickness.

transferred to *Antrophyum*. This species is known only from the type specimen in MA, which, unfortunately, is only the top part of what appears to have been a very large frond. We could not exclude the possibility that *A. rigidum* ined. is conspecific with *A. callifolium* and future studies should attempt to include a specimen from the type locality to test this hypothesis. If they turn out to be the same species, the name *A. rigidum* would have priority over *A. callifolium*. However, considering that *A. callifolium* has been widely used for a long time, proposing to conserve *A. callifolium* against *A. rigidum* may be a wiser choice in terms of taxonomic stability.

Notably, we included two specimens originally identified as *A. callifolium* in the phylogenetic analysis that were resolved as only distantly related to *A. callifolium* (*A.* aff. *callifolium* from the Philippines in Fig. 3). We cannot find any reliable morphological character to separate these two specimens from *A. callifolium*, but the large genetic distance suggests that these should be recognized as a distinct species. Future studies should include more specimens from the Philippines and type localities of members of the *A. reticulatum* complex.

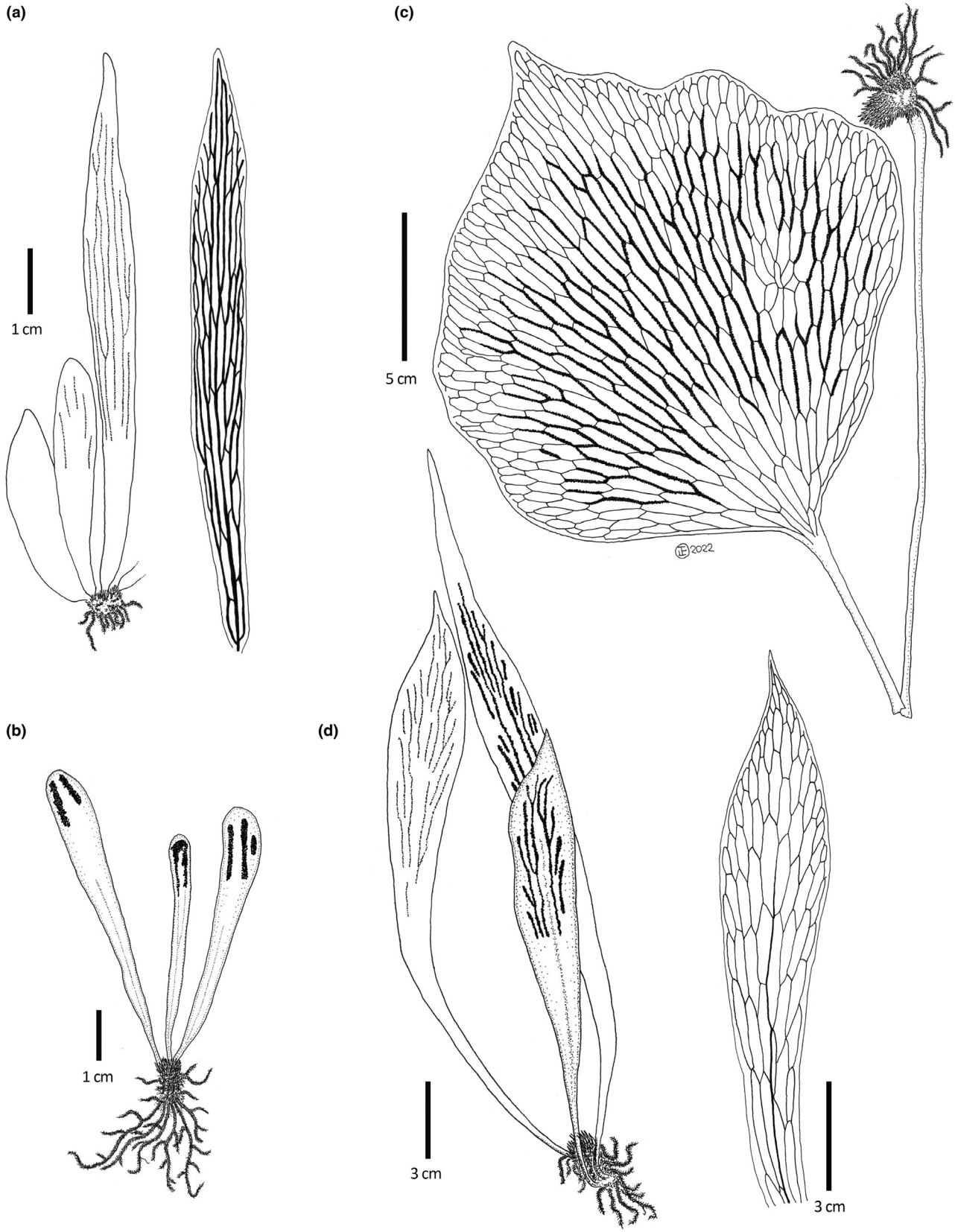

Fig. 10. Illustrations of the four newly described species. (a) *Antrophyum crassifolium*, (b) *Antrophyum kinabaluense*, (c) *Antrophyum pseudolatifolium* and (d) *Antrophyum tahitense*.

Doing so would enable testing whether this species fits any published names in the *A. reticulatum* complex or is an undescribed species.

Antrophyum semicostatum Blume (type from Java) is among the earliest published names of the genus and is widely distributed throughout Malesia (Indonesia, Malaysia, Papua New Guinea and the Philippines). When Blume (1828) described the species, he informally recognized one additional variety to show the lamina shape variation he observed. Both the type variety and his var. "*B*" have lanceolate fronds but the apical portion of the type variety is dilated while that of the variety "*B*" is not. Three other varieties of *A. semicostatum* were described subsequently (van Alderwerelt van Rosenburgh, 1911, 1912; Ito, 1975), again, indicating the high morphological variation of this species. Variety *sarawakense* H.Ito (type from Sarawak) is diagnosed by having obovate fronds (vs. oblanceolate); var. *marthae* Alderw. (type from New Guinea) is diagnosed by having pyriform paraphyses (vs. clavate); and var. *caudatum* Alderw. (type from Java, not found). In this study, we included four specimens of *A. semicostatum* in the phylogenetic analysis (two each from Java and Sabah, although labelled Indonesia and Malaysia in Fig. 3) and found a large genetic distance among them (Fig. 3, clade C-4). Specifically, the two specimens from Java (V022, V146) representing the type variety are genetically distant from the other two specimens from Sabah (V429, V500), which have similar lamina shapes to var. *sarawakense*. The large genetic distance between these two clades indicates limited gene flow between the populations, and thus might justify the recognition of var. *sarawakense* as a distinct species, especially when considering that the distance is much larger than those found between many sister species (e.g. *A. formosanum* Hieron. vs. *A. henryi* Hieron., *A. plicatum* Fée vs. *A. vittarioides*). However, as mentioned, lamina shape is not a good character to distinguish them and specimens with intermediate morphology are not rare. We therefore refrain from revising their taxonomy until a useful morphological delimitation between them is found. Future studies should include more specimens, especially those representative of the types of the varieties to clarify their phylogenetic relationship and taxonomy.

New synonymies

Antrophyum plantagineum (Cav.) Kaulf. (type from the Philippines) and *A. angustatum* Brack. (type from Samoa but erroneously cited as Tahiti in the protologue, Florence pers. comm.; Rouhan et al., 2008) are morphologically similar species. Both species have falcate fronds with distinct stipes. Most previous studies distinguished these two species by frond size, those of *A. angustatum* being narrower and longer than those of *A. plantagineum* (Christensen, 1943). *Antrophyum plantagineum* is widely distributed from South Asia (India, Sri Lanka), Malesia (widely distributed), Australia and the Pacific Islands (widely distributed), whereas *A. angustatum* is restricted only to Samoa. Moore (1857) was the first to notice the similarity of the two species and placed *A. angustatum* as a variety of *A. plantagineum*. In this study, we included nine specimens of *A. plantagineum* and four of *A. angustatum* in the morphological analysis. Our results concur with the previous finding that frond length and length/width ratio can be used to distinguish the two species (Table S1). However, the results of the molecular phylogenetic analysis tell a different story. We included six specimens of *A. plantagineum* and one of *A. angustatum* in the molecular phylogenetic analyses. These specimens were resolved into three clades with a stronger geographic pattern than a morphological one. Specifically, four specimens from the Pacific Islands, including one *A. angustatum* (V468) and three *A. plantagineum* (V248, V350, V385), formed a clade; the two specimens from the Philippines (V227, V363) formed another clade; a specimen from Indonesia (V623) formed its own clade (Fig. 3). In other words, *A. angustatum* was nested in *A. plantagineum* and might be just a local form of *A. plantagineum* with narrowed laminae. We therefore synonymize *A. angustatum* under *A. plantagineum*.

Antrophyum strictum Mett. and *A. megistophyllum* Copel. are another pair of morphologically similar species. The former was described from New Guinea based on a collection with long oblanceolate fronds (27 × 5 cm) whereas the latter was described based on a much larger plant (69 × 17 cm) from the Solomon Islands. After examining more specimens from Papuasia, we found that the frond sizes of specimens from both areas are variable and often overlap. For example, *Chen et al. SITW00408* (V315, from the Solomon Islands) has fully fertile fronds that are not much larger than the type of *A. strictum* (31 × 3 cm). Furthermore, we could not find any obvious difference in their paraphyses or rhizome scales. Phylogenetically, the four included specimens showed a geographic pattern and a slight genetic distance was found between the specimens from Papua New Guinea (V323, V464) and the Solomon Islands (V250, V315). Two scenarios might explain our findings. First, the populations from the two areas are at the early stage of diverging and accompanying morphological differentiation has yet to form. Second, our current sampling is biased and does not reflect the real genetic diversity of both areas. Since we were unable to find a reliable morphological trait to distinguish them, we tentatively accept only one species, with *A. strictum* having priority.

Antrophyum subfalcatum Brack. was described from Fiji and diagnosed, in part, by its narrowly falcate fronds. *Antrophyum smithii* C.Chr. was also described from Fiji and a close affinity with *A. semicostatum* had been proposed by Christensen (in Smith, 1936). Chen et al. (2015) was the first to show a morphological similarity and a close phylogenetic affinity between *A. subfalcatum* and *A. smithii*. Most previous studies distinguished these two species by frond shape (Brownlie, 1977; National Museum of Nature and Science (NMNS), 2008; Chen et al., 2017). This is true when comparing only their type collections. Specifically, those of *A. smithii* are long oblanceolate but not falcate whereas those of *A. subfalcatum* are linear to narrowly oblanceolate and falcate. However, such differences fade away when more specimens are included based on our herbarium observations. In this study, we include eight specimens covering both morphological variation (with specimens representing the types of both species) and geographic distribution for both species. These eight specimens show only a little genetic variation and there is no correlation between the morphology and genetic variation. As a result, we conclude that these two names are synonyms with *A. subfalcatum* having priority.

New species

Based on our herbarium studies, we propose recognizing four new species with distinct morphologies, namely *A. crassifolium* C.W.Chen, *A. kinabaluense*, *A. pseudolatifolium* C.W.Chen and *A. tahitense* C.W.Chen & J.H.Nitta. *Antrophyum crassifolium* is diagnosed by the combination of small plant size, thick laminae and narrowly oblong paraphyses (Fig. 5). *Antrophyum kinabaluense* is diagnosed by having tiny linear fronds (Fig. 4). *Antrophyum pseudolatifolium* is very similar to *A. latifolium*. Both have large and broadly obovate fronds (Fig. 4), but the former has globose paraphyses (Fig. 5), whereas the latter has narrowly oblong ones (Fig. 5). *Antrophyum tahitense* is similar to *A. solomonense* in terms of gross morphology but can be distinguished by having different paraphyses (globose vs. clavate, Fig. 5). In addition to the morphological differences, we were able to test the phylogenetic relationships of *A. crassifolium*, *A. pseudolatifolium* and *A. tahitense*. We found that each species occupied a unique placement on the phylogenetic tree. Specifically, *A. crassifolium* was resolved as the only species of clade B-1 (Fig. 3). *Antrophyum pseudolatifolium* was resolved as sister to clade C-2 that comprises *A. castaneum* H.Itô and *A. obovatum* (Fig. 3). *Antrophyum tahitense* was resolved as sister to the group of *A. austroqueenslandicum* and *A. solomonense* (Fig. 3). Furthermore, in cases where multiple specimens were included, all specimens formed a clade. Overall, both morphological and molecular evidence support the recognition of these new species. We therefore formally describe them in the taxonomy section.

Species without molecular data

Of the 34 species tentatively recognized in this study, we were unable to include three (i.e. *A. kinabaluense*, *A. marginale* and *A. simulans*) in our phylogenetic analyses owing to a lack of material. It will be interesting to include them in future analyses, but we meanwhile hypothesize their phylogenetic relationships based on morphological comparisons. The tiny plant size, with fronds ca. 2 cm long and 0.3 cm wide, is the most striking feature of *A. kinabaluense*. So far, this species is only known by two collections from Sabah, Malaysia, probably from the same locality. The only other species with comparable frond size is *A. nanum* Fée. According to the analysis of character evolution, the reduction of frond size occurred at least twice in *Antrophyum*, once in the *A. immersum*/*nanum* clade and the other in the *A. formosanum*/*henryi* clade (Fig. 9). We therefore predict that *A. kinabaluense* has a close affinity with *A. nanum* because not only are both small plants, but they also share capitate paraphyses (rather than taeniform paraphyses as in the *A. formosanum*/*henryi* clade). This hypothesis is further supported by the overlapping distribution of *A. kinabaluense* and *A. nanum*, both being recorded in Sabah.

As mentioned earlier, *A. marginale* and *A. brookei* have fronds of a similar shape but with sori arranged differently. These two species also have different distributions. *A. marginale* is only recorded from Java whereas *A. brookei* is only recorded from Borneo. The sori feature of *A. marginale* (i.e. two marginal soral lines that only a little shorter than the frond) is unique among the species with filiform paraphyses, suggesting that it is a distinct species but with a close affinity to the *A. reticulatum* complex.

Antrophyum simulans is only known by the type collection from Java, Indonesia. It stands out from the species with capitate paraphyses by the combination of fusiform shaped fronds with long stipes and narrowly oblong paraphyses. Narrowly oblong paraphyses is a rare trait in *Antrophyum* and only found in two other species, *A. crassifolium* and *A. latifolium*. Morphologically, *A. simulans* is more similar to *A. latifolium* in having the long-stiped fronds. They further have overlapping distribution and thus are probably closely related.

Description of new species

Antrophyum crassifolium C.W.Chen, sp. nov. Figs 4, 5, 6, 10a. Differs from its congeners by having very

thick laminae and soral paraphyses with narrowly oblong apical cells.

Habit unknown—Rhizome short-creeping, scaly; scales clathrate, linear-lanceolate, ca. 2.5 × 0.3 mm at the base, tapering to one cell wide at the apex, brown, margin denticulate, cell walls 13–17 μm thick. Fronds approximately clustered; without obvious stipes; laminae strongly coriaceous, narrowly oblanceolate, ca. 12 × 1 cm, broadest in the upper two-thirds, tapering to the base, the midribs not visible. Sori linear, in deep grooves, covering most of the laminae except near the base, seldom reticulate; paraphyses capitate, ca. four cells long, unbranched, apical cell narrowly oblong, 40–80 × 15–35 μm. Spores tetrahedral.

Holotype—PAPUA NEW GUINEA. Morobe Province, Markham Valley, ca. 300–600 m (1000–2000 ft), 30 November 1939, *M. S. Clemens 10848* (UC no. 632534!, isotype UC no. 660617!).

Etymology—From the Latin *crassus*, thick, and *-folius*, leaf, referring to the coriaceous texture of the lamina.

Habitat—Forests at ca. 300–600 m.

Note—This species is known only by the type collection.

Antrophyum kinabaluense C.W.Chen, sp. nov. Figs 4, 5, 6, 10b. Most similar to *A. nanum* but differs from that species by having linear fronds with only two or three short soral lines near apices (vs. 4 or more soral lines).

Epiphytic—Rhizome short-creeping, scaly; scales clathrate, linear-lanceolate, ca. 1.7 × 0.4 mm at the base, tapering to one cell wide at the apex, brown, margin denticulate, cell walls 11–20 μm thick. Fronds approximately clustered; without obvious stipes; laminae thinly coriaceous, short linear, ca. 2 × 0.3 cm, the midribs obscure. Sori linear, two (to three) on each frond, in shallow grooves; paraphyses capitate, two to three cells long, unbranched, apical cell globose. Spores tetrahedral.

Holotype—MALAYSIA. Sabah, Kota Belud, Sayap, Kinabalu Park, 900 m, *D. Sumbin & J. Gisii SP07774* (SNP!).

Etymology—Named after the type locality, Kinabalu Park in Sabah, Malaysia.

Habitat—Hill dipterocarp forests at 870–900 m.

Additional specimens—MALAYSIA. Sabah, Kota Belud, Sayap, Kinabalu Park, Kimantis Trail, 870 m, 6 June 1992, *R. Jaman 4048* (SNP!).

Note—The phylogenetic placement of this species is still unknown, but based on the morphology (see the Discussion), it probably has a close affinity with *A. nanum*.

Antrophyum pseudolatifolium C.W.Chen, sp. nov. Figs 4, 5, 6, 10c. Very similar to *A. latifolium* but differs from that species in having soral paraphyses with globose (vs. narrowly oblong) apical cells.

Lithophilic—Rhizome short-creeping, scaly; scales clathrate, linear-lanceolate, 3.5–5 × 0.5–1 mm at the base, tapering to one cell wide at the apex, brown, margin strongly denticulate, cell walls 10–20 μm thick. Fronds approximately clustered; stipes long, about the same as to twice the laminae length, rounded in cross-section; laminae sub-coriaceous, very widely obovate, 15–30 × 10–25 cm excluding stipe, broadest near the middle, the midribs obscure. Sori linear, in shallow grooves, reticulate; paraphyses capitate; four to six cells long, branched, apical cell globose. Spores tetrahedral.

Holotype—PHILIPPINES. Mindanao, Davao del Sur Province, Mt Apo, 1920 m, 4 May 2012, *L.-Y. Kuo 2544* (TAIF no. 483873!, isotypes TAIF no. 483872!, 483874!, 483876!).

Etymology—From the Greek *pseudo*, false; referring to the close resemblance between this species and *A. latifolium*.

Habitat—Primary rain forests at 1500–1920 m, usually near streams or waterfalls.

Additional specimens—MALAYSIA. Sabah, Mount Kinabalu, Penibukan, by waterfalls, ca. 1500–1800 m (5000–6000 ft), 23 October 1953, *J. & M. S. Clemens 40294 & 40963* (UC no. 560484!).

PHILIPPINES. Mindanao, Mt Apo, May 1909, *A. D. E. Elmer 10729* (BO no. 1426446!). Mindanao, Mt Matutum, May 1917, *E. B. Copeland s.n.* (UC no. 352511!). Mindanao, Davao del Sur Province, Mt Apo, Mandarangan trail entrance, 1720–1920 m, 4 May 2012, *L.-Y. Kuo 2544* (TAIF no. 483872!, 483873!, 483874!, 483876!).

Antrophyum tahitense C.W.Chen & J.H.Nitta, sp. nov. Figs 4, 5, 6, 10d. Similar to *A. solomonense* but differs from that species by its smaller size (frond length 15–30 vs. 8–20 cm) and having soral paraphyses with globose (vs. clavate) apical cells.

Epiphytic or lithophilic—Rhizome short-creeping, scaly; scales clathrate, linear-lanceolate, 4.5–6.5 × 0.6–1 mm at the base, tapering to one cell wide at the apex, brown, margin denticulate, cell walls 13–24 μm thick. Fronds approximately clustered; stipes short, less than one-fifth the length of the frond; laminae subcoriaceous, oblanceolate, 8–23 × 3–4 cm, broadest in the upper two-thirds, tapering to base, the midribs visible. Sori linear, superficial, seldom reticulate; paraphyses capitate, three to five cells long, branched, apical cell globose. Spores tetrahedral.

Holotype—FRENCH POLYNESIA. Tahiti, S. of Orohena, on trees, frequent, 1400 m, 16 May 1927, *L. H. MacDaniels 1455* (UC no. 465109!).

Etymology—The epithet *tahitense* refers to the provenance of the type collection.

Habitat—Damp forests at 300–1400 m.

Additional specimens—FRENCH POLYNESIA. Tahiti, Lake Vaheria, on dry rocks, occasional, 500 m, 3 June 1927, *L. H. MacDaniels 1610* (UC no. 465114!). Tahiti, Papara, 31 km from Papeete, moist rocks, frequent, 400 m, 28 June 1927, *L. H. MacDaniels 1720* (UC no. 465110!, 465112!). Tahiti, Ridge to Aorai, 1203 m (3950 ft), 5 June 1930, *M. L. Grant 3749* (UC no. 437817!). Tahiti, Ronui, 980 ft, 1 July 1930, *M. L. Grant 3892A* (UC no. 437822!). Tahiti, Orofena, 716–777 m (2350–2550 ft), 21 September 1930, *M. L. Grant 4198* (UC no. 437826!). Moorea, Mt Tohiea, 1000 m, 3 August 2012, *J. Nitta 1450* (UC!).

Note—Three *Antrophyum* species have been recorded in French Polynesia so far: *A. plantagineum*, *A. reticulat um* and *A. tahitense*. *Antrophyum tahitense* differs from *A. reticulatum* by having capitate paraphyses (vs. filiform). *Antrophyum tahitense* can be further dist inguished from *A. plantagineum* by having larger capit ate paraphyses (mean width ca. 110 μm vs. ca. 60 μm). Furthermore, *A. tahitense* is found at higher elevations (to 1400 m) than the other two species which typically occur at lower elevations (below 500 m).

A key to the 34 species of Antrophyum

In this study, we tentatively recognize 34 species by integrating the evidence from the morphology, phylogeny and ecology. Among the 34 species, *A.* aff. *callifolium* cannot be distinguished from *A. callifolium* by morphology and thus they are keyed to the same place (see the Discussion). We separate the species into three groups based on the three main types of the apical cell of soral paraphyses (referred to as simply paraphyses throughout the key).

Group 1. Paraphyses filiform, more than 500 μm long, <30 μm wide.

1a. Fronds linear, length/width ratio ca. 30 ..... 2.
1b. Fronds not linear, length/width ratio <20 .... 4.
2a. Rhizome scale cell walls 15–25 μm ... ***A. vittarioids***.
2b. Rhizome scale cell walls 10–15 μm .... 3.
3a. Soral lines three to six, less than half the length of frond ..... ***A. brookei***.
3b. Soral lines two, only slightly shorter than frond ..... ***A. marginale***.
4a. Fronds narrowly oblanceolate, length/width ratio 10–20 ... 5.
4b. Fronds oblanceolate, length/width ratio <10 ... 7.
5a. Plant from Madagascar ... ***A. malgassicum***.
5b. Plant from Asia, Malesia, or Pacific Islands ... 6.
6a. Fronds <20 cm long, paraphyses 0.7–1.3 mm long ... ***A. hovenkampii***.
6b. Fronds more than 20 cm long, paraphyses <0.5 mm long ... ***A. sessilifolium***.
7a. Rhizome scale cell walls 25–35 μm ... ***A. reticulatum***.
7b. Rhizome scale cell walls 10–20 μm ... 8.
8a. Fronds with distinct stipes ... ***A. annamense***.
8b. Fronds without distinct stipes ..... 9.
9a. Laminae chartaceous, plant from a tropical area ... ***A. callifolium*** and ***A.* aff. *callifolium***.
9b. Laminae coriaceous, plant from the Himalayas ... ***A. plicatum***.

Group 2. Paraphyses taeniform, 160–400 μm long, more than 35 μm wide.

1a. Fronds 0.5–1.5 cm wide .... ***A. henryi***.
1b. Fronds 2.5–4 cm wide ... 2.
2a. Fronds 10–25 cm long, paraphyses 300–400 μm long ... ***A. formosanum***.
2b. Fronds 15–30 cm long, paraphyses 160–200 μm long ... ***A. nambanense***.

Group 3. Paraphyses capitate, 60–150 μm long, 40–100 μm wide.

1a. Fronds obovate, orbicular, or rhomboid, with long distinct stipes ... 2.
1b. Fronds linear or oblanceolate, with or without distinct stipes ... 5.
2a. Paraphyses narrowly oblong ..... ***A. latifolium***.
2b. Paraphyses globose ... 3.
3a. Paraphyses 100–200 μm long ... ***A. obovatum***.
3b. Paraphyses 50–120 μm long ..... 4.
4a. Fronds more than 30 cm long, orbicular ... ***A. pseudolatifolium***.

4b. Fronds <30 cm long, rhomboid ... ***A. ledermannii***.
5a. Fronds <10 cm long ... 6.
5b. Fronds more than 10 cm long ... 7.
6a. Fronds with only two or three short soral lines near apices ... ***A. kinabaluense***.
6b. Fronds with four or more soral lines ... ***A. nanum***.
7a. Paraphyses narrowly oblong ... 8.
7b. Paraphyses clavate, globose or oblate ... 9.
8a. Fronds fusiform, with distinct stipes, laminae chartaceous ... ***A. simulans***.
8b. Fronds oblanceolate, without distinct stipes, laminae strongly coriaceous ... ***A. crassifolium***.
9a. Paraphyses oblate, width greater than length ... ***A. brassii***.
9b. Paraphyses clavate or globose ... 10.
10a. Paraphyses clavate, length greater than width ... 11.
10b. Paraphyses globose, length and width about the same ... 15.
11a. Both clavate and boot-shaped paraphyses present ... 12.
11b. Only clavate paraphyses present ... 13.
12a. Fronds linear, about 1 cm wide ... ***A. austroqueenslandicum***.
12b. Fronds oblanceolate, about 2 cm wide ... ***A. solomonense***.
13a. Rhizome scale cell walls 8–12 μm ... ***A. castaneum***.
13b. Rhizome scale cell walls 12–17 μm ... 14.
14a. Fronds narrowly oblanceolate, with distinct stipes ... ***A. elongatum***.
14b. Fronds oblanceolate, without distinct stipes ... ***A. semicostatum***.
15a. Paraphyses 100–300 μm long ... 16.
15b. Paraphyses 50–150 μm long ... 17.
16a. Laminae coriaceous, plant from New Caledonia ... ***A. novae-caledoniae***.
16b. Laminae chartaceous, plant from French Polynesia ... ***A. tahitense***.
17a. Fronds more than 40 cm long ... ***A. strictum***.
17b. Fronds <30 cm long ... 18.
18a. Fronds with distinct stipes ... ***A. plantagineum***.
18b. Fronds without distinct stipes ... 19.
19a. Fronds narrowly oblanceolate, more than 20 cm long ... ***A. subfalcatum***.
19b. Fronds oblanceolate, <20 cm long ... ***A. immersum***.

Acknowledgements

This study is part of the doctoral dissertation of CWC. We greatly appreciate the following herbarium curators and staff who made their invaluable specimens available to us: Anthony Brach (A), Brigitte Zimmer (B), Alison Paul (BM), Arief Hidayat (BO), Anna Haigh (K), Richard C. K. Chung (KEP), Kien Thai Yong (KLU), Hidetoshi Nagamasu (KYO), Nicolien Sol (L), Hans-Joachim Esser (M), Brad Ruhfel (MICH), James C. Solomon (MO), Xian-Chun Zhang (PE), Andi Maryani A. Mustapeng (SAN), Runi Pungga (SAR), David Middleton (SING), Jamili Nais (SNP), Hui Wang (SZG), Akiko Shimizu (TI), Shih-Wen Chung (TAIF), Atsushi Ebihara (TNS), Alan Smith (UC), and Eric Schuettpelz (US). We particularly thank David Middleton, Li-Bing Zhang, Li-Yaung Kuo, Michael Kessler and Ping-Fong Lu for sharing their collections, and two anonymous reviewers for their valuable suggestions. Parts of this project were supported by grants from Academia Sinica to KFC.

Conflict of interest

None declared.

Data availability statement

The raw morphological measurements of this study are available at MorphoBank: morphobank.org/permalink/?P4644. The DNA sequence data are openly available in the GenBank Nucleotide Database at https://www.ncbi.nlm.nih.gov/genbank, and all accession numbers are provided in Table S1. DNA sequences alignments used for phylogenetic analyses are available upon request. The codes for biogeographical analyses are openly available at https://github.com/joelnitta/antrophyum_ow.

References

Adams, D., Collyer, M., Kaliontzopoulou, A. and Baken, E., 2021. Geomorph: software for geometric morphometric analyses. R package version 4.0.2.
van Alderwerelt van Rosenburgh, C.R.W.K., 1911. New or interesting Malayan ferns 3. Bull. Jard. Bot. Buit. II 1, 1–29.
van Alderwerelt van Rosenburgh, C.R.W.K., 1912. New or interesting Malayan ferns 4. Bull. Jard. Bot. Buit. II 7, 1–41.
Álvarez-Molina, A. and Cameron, K.M., 2009. Molecular phylogenetics of *Prescottiinae* s.l. and their close allies (Orchidaceae, Cranichideae) inferred from plastid and nuclear ribosomal DNA sequences. Am. J. Bot. 96, 1020–1040.
Benedict, R.C., 1907. The genus *Antrophyum* – I. synopsis of subgenera, and the American species. Bull. Torrey Bot. Club 34, 445–458.
Benedict, R.C., 1911. The genera of the fern tribe Vittarieae: their external morphology, venation and relationships. Bull. Torrey Bot. Club 38, 153–190.
Blomberg, S.P., Garland, T., Jr. and Ives, A.R., 2003. Testing for phylogenetic signal in comparative data: behavioral traits are more labile. Evolution 57, 717–745.

Blume, C.L., 1828. Enumeratio plantarum Javae et insularum adjacentium, fasc. II, Filices. Apud J. W. van Leeuwen, Lugduni Batavorum.

Bory de St Vincent, J.B.G.M., 1804. Voyage dans les Quatre Principales Îles des Mers d'Afrique. Tome Second, Paris.

Bouckaert, R., Vaughan, T.G., Barido-Sottani, J., Duchêne, S., Fourment, M., Gavryushkina, A., Heled, J., Jones, G., Kühnert, D., De Maio, N., Matschiner, M., Mendes, F.K., Müller, N.F., Ogilvie, H.A., du Plessis, L., Popinga, A., Rambaut, A., Rasmussen, D., Siveroni, I., Suchard, M.A., Wu, C.H., Xie, D., Zhang, C., Stadler, T. and Drummond, A.J., 2019. BEAST 2.5: an advanced software platform for Bayesian evolutionary analysis. PLoS Comput. Biol. 15, e1006650.

Brackenridge, W.D., 1854. United States exploring expedition, during the years 1838, 1839, 1840, 1841, 1842, under the command of Charles Wilkes, U.S.N. Vol. 16: Botany, cryptogamia, filices, including Lycopodiaceae and Hydropterides. C. Sherman, Philadelphia, PA.

Brownlie, G., 1977. The pteridophyte flora of Fiji. Bramer, Vaduz.

Brummitt, R.K., 2001. World geographical scheme for recording plant distributions, 2nd edition. Carnegie Mellon University, Hunt Institute for Botanical Documentation, Pittsburgh, PA.

Burnham, K.P. and Anderson, D.R., 1998. Model selection and inference. Springer, New York.

Cámara-Leret, R., Frodin, D.G., Adema, F., Anderson, C., Appelhans, M.S., Argent, G., Arias Guerrero, S., Ashton, P., Baker, W.J., Barfod, A.S., Barrington, D., Borosova, R., Bramley, G.L.C., Briggs, M., Buerki, S., Cahen, D., Callmander, M.W., Cheek, M., Chen, C.W., Conn, B.J., Coode, M.J.E., Darbyshire, I., Dawson, S., Dransfield, J., Drinkell, C., Duyfjes, B., Ebihara, A., Ezedin, Z., Fu, L.F., Gideon, O., Girmansyah, D., Govaerts, R., Fortune-Hopkins, H., Hassemer, G., Hay, A., Heatubun, C.D., Hind, D.J.N., Hoch, P., Homot, P., Hovenkamp, P., Hughes, M., Jebb, M., Jennings, L., Jimbo, T., Kessler, M., Kiew, R., Knapp, S., Lamei, P., Lehnert, M., Lewis, G.P., Linder, H.P., Lindsay, S., Low, Y.W., Lucas, E., Mancera, J.P., Monro, A.K., Moore, A., Middleton, D.J., Nagamasu, H., Newman, M.F., Nic Lughadha, E., Melo, P.H.A., Ohlsen, D.J., Pannell, C.M., Parris, B., Pearce, L., Penneys, D.S., Perrie, L.R., Petoe, P., Poulsen, A.D., Prance, G.T., Quakenbush, J.P., Raes, N., Rodda, M., Rogers, Z.S., Schuiteman, A., Schwartsburd, P., Scotland, R.W., Simmons, M.P., Simpson, D.A., Stevens, P., Sundue, M., Testo, W., Trias-Blasi, A., Turner, I., Utteridge, T., Walsingham, L., Webber, B.L., Wei, R., Weiblen, G.D., Weigend, M., Weston, P., de Wilde, W., Wilkie, P., Wilmot-Dear, C.M., Wilson, H.P., Wood, J.R.I., Zhang, L.B. and van Welzen, P.C., 2020. New Guinea has the world's richest Island flora. Nature 58, 579–583.

Cavanilles, A.J., 1802. Descripción de las plantas. Imprenta Real, Madrid.

Chen, C.-W., Huang, Y.-M., Kuo, L.-Y., Nguyen, Q.D., Luu, H.T., Callado, J.R., Farrar, D.R. and Chiou, W.-L., 2013. *TrnL-F* is a powerful marker for DNA identification of field vittarioid gametophytes (Pteridaceae). Ann. Bot. 111, 663–673.

Chen, C.-W., Nitta, J.H., Fanerii, M., Yang, T.-Y.A., Pitisopa, F., Li, C.-W. and Chiou, W.-L., 2015. *Antrophyum solomonense* (Pteridaceae), a new species from the Solomon Islands, and its systematic position based on phylogenetic analysis. Syst. Bot. 40, 645–651.

Chen, C.-W., Lindsay, S., Kuo, L.-Y., Fraser-Jenkins, C.R., Ebihara, A., Luu, H.T., Park, C.W., Chao, Y.-S., Huang, Y.-M. and Chiou, W.-L., 2017. A systematic study of east Asian vittarioid ferns (Pteridaceae, Vittarioideae). Bot. J. Linn. Soc. 183, 545–560.

Chen, C.-W., Lindsay, S., Yong, K.T., Mustapeng, A.M.A., Amoroso, V.B., Dang, V.D. and Huang, Y.-M., 2019. Clarification of two poorly known vittarioid ferns (Pteridaceae): *Haplopteris angustissima* and *H. capillaris*. Syst. Bot. 44, 483–493.

Chen, C.-W., Dang, M.T., Luu, H.T., Kao, T.-T., Huang, Y.-M. and Li, C.-W., 2020. *Antrophyum nambanense*, a new vittarioid fern (Pteridaceae; Polypodiales) from Vietnam. Syst. Bot. 45, 450–459.

Chen, C.-W., Chao, Y.-S., Andi, M.A.M., Sapawi, N.M. and Huang, Y.-M., 2021. Two new fern species from Gunung Mulu National Park, Sarawak, Malaysia. Syst. Bot. 46, 573–581.

Chen, C.-W., Perrie, L., Glenny, D., Chiou, W.-L., Fawcett, S., Smith, A.R., Parris, B.S., Ebihara, A., Ohlsen, D., Lehtonen, S., Dong, S.-Y., Lenhert, M., Field, A., Chao, Y.-S., Murdock, A.G. and Sundue, M., 2022. An annotated checklist of lycophytes and ferns of the Solomon Islands. Fern Gaz. 21, 292–317.

Christ, K.H.H., 1907. Spiciligium filicum Philippinensium novarorum aut imperfecte cognitarum. Philipp. J. Sci. 2, 186–187.

Christensen, C., 1905–1906. Index filicum. H. Hagerup, Copenhagen.

Christensen, C., 1926. Fougères de Madagascar récoltes de M.H. Perrier de la Bathie. Notes Ptéridol. 16, 11–153.

Christensen, C., 1943. A revision of the Pteridophyta of Samoa. Bulletin 177. Bernice P. Bishop Museum, Honolulu.

Condamine, F.L., Leslie, A.B. and Antonelli, A., 2017. Ancient islands acted as refugia and pumps for conifer diversity. Cladistics 33, 69–92.

Crane, E., 1997. A revised circumscription of the genera of the fern family Vittariaceae. Syst. Bot. 22, 509–517.

Crane, E., Farrar, D. and Wendel, J., 1995. Phylogeny of the Vittariaceae: convergent simplification leads to a polyphyletic *Vittaria*. Am. Fern J. 85, 283–305.

Dupin, J., Matzke, N.J., Särkinen, T., Knapp, S., Olmstead, R.G., Bohs, L. and Smith, S.D., 2017. Bayesian estimation of the global biogeographical history of the Solanaceae. J. Biogeogr. 44, 887–899.

Edgar, R.C., 2004. MUSCLE: multiple sequence alignment with high accuracy and high throughput. Nucleic Acids Res. 32, 1792–1797.

Fée, A.L.A., 1852. Histoire des Antrophyées: Quatrième mémoire. In: Mémoires sur la Famille des Fougères. J.B.Baillière and V.Masson, Paris.

Forster, J.G.A., 1786. Florulae Insularum Australium Prodromus. Dieterich, Göttingen.

Fraser-Jenkins, C.R., Gandhi, K.N., Kholia, B.S. and Benjamin, A., 2017. An annotated checklist of Indian Pteridophytes, Part 1. Bishen Singh Mahendra Pal Singh, Dehra Dun.

Hall, T.A., 1999. BioEdit: a user-friendly biological sequence alignment editor and analysis program for windows 95/98/NT. Nucleic Acids Symp. Ser. 41, 95–98.

Holttum, R.E., 1955 ['1954']. A revised flora of Malaya: an illustrated systematic account of the Malayan flora, including commonly cultivated plants, Vol. 2. Ferns of Malaya. Government Printing Office, Singapore.

Hooker, W.J., 1861. A second century of ferns. W. Pamplin, London.

Hooker, W.J. and Greville, R.K., 1828. Icones filicum, Vol. 1. Richard Taylor, London.

Ito, H., 1975. Ferns of Borneo, collected by M. Hirano and M. Hotta 7. Acta Phytotax. Geobot. 26, 149–151.

Kaulfuss, G.F., 1824. Enumeratio filicum. Sumtibus Caroli Cnobloch, Lipsiae.

Kunze, G., 1848. In filices Javae Zollingerianas observationes continuatae Kunzii, Lipsiensis (Fortsetzung). Bot. Zeitung (Berlin) 6, 141–146.

Landis, M.J., Matzke, N.J., Moore, B.R. and Huelsenbeck, J.P., 2013. Bayesian analysis of biogeography when the number of areas is large. Syst. Biol. 62, 789–804.

Lanfear, R., Frandsen, P., Wright, A. and Senfeld, T., 2017. PartitionFinder 2: new methods for selecting partitioned models of evolution for molecular and morphological phylogenetic analyses. Mol. Biol. Evol. 34, 772–773.

Larsson, A., 2014. AliView: a fast and lightweight alignment viewer and editor for large data sets. Bioinformatics 30, 3276–3278.

Li, F.W., Kuo, L.Y., Huang, Y.M., Chiou, W.L. and Wang, C.N., 2010. Tissue-direct PCR, a rapid and extraction-free method for barcoding of ferns. Mol. Ecol. Resour. 10, 92–95.
Lindsay, S. and Middleton, D.J., 2020. Adiantaceae. In: Parris, B.S., Kiew, R., Chung, R.C.K. and Cheah, Y.H. (Eds.), Flora of Peninsular Malaysia Ser. 1, Vol. 3. Forest Research Institute Malaysia, Kepong, pp. 113–155.
Matzke, N., 2013. BioGeoBEARS: BioGeography with Bayesian (and Likelihood) evolutionary analysis in R scripts. University of California, Berkeley, CA.
Moore, T., 1857. Index filicum. Pamplin, London.
National Museum of Nature and Science (NMNS) (Eds.). 2008. Illustrated Flora of Ferns and Fern Allies of South Pacific Islands. National Museum of Nature and Science Book Series No. 8. Tokai University Press, Tokyo.
Pagel, M., 1999. Inferring the historical patterns of biological evolution. Nature 401, 877–884.
Park, S.H., Kim, J.S. and Kim, H.T., 2020. Study of the independent gametophytes found on Jeju Island in South Korea and the first record of the obligate independent gametophyte of *Antrophyum obovatum* baker. Ecol. Evol. 10, 7826–7838.
Park, S.H., Kim, J.S. and Kim, H.T., 2021. A small number of gametophytes with gametangia and stunted sporophytes of *Antrophyum obovatum* Baker (Pteridaceae): the suppression of functional sporophyte production by prezygotic and postzygotic sterility. Plan. Theory 10, 170.
Pillon, Y., Jaffré, T., Birnbaum, P., Bruy, D., Cluzel, D., Ducousso, M., Fogliani, B., Ibanez, T., Jourdan, H., Lagarde, L., Léopold, A., Munzinger, J., Pouteau, R., Read, J. and Isnard, S., 2021. Infertile landscapes on an old oceanic island: the biodiversity hotspot of New Caledonia. Biol. J. Linn. Soc. 133, 317–341.
Plunkett, G.M., Ranker, T.A., Sam, C. and Balick, M.J., 2022. Preliminary checklist of the Vascular Flora of Vanuatu. Available at: https://mail.pvnh.net/?page=checklist (accessed 30 June 2022).
Pouteau, R., Trueba, S., Felid, T.S. and Isnard, S., 2015. New Caledonia: a Pleistocene refugium for rain forest lineages of relict angiosperms. J. Biogeogr. 42, 2062–2077.
PPG I, 2016. A community-derived classification for extant lycophytes and ferns. J. Syst. Evol. 54, 563–603.
R Core Team, 2017. R: A language and environment for statistical computing. R Foundation for Statistical Computing, Vienna.
Rambaut, A., Drummond, A.J., Xie, D., Baele, G. and Suchard, M.A., 2018. Posterior summarisation in Bayesian phylogenetics using tracer 1.7. Syst. Biol. 67, 901–904.
Ree, R.H. and Smith, S.A., 2008. Maximum likelihood inference of geographic range evolution by dispersal, local extinction, and cladogenesis. Syst. Biol. 57, 4–14.
Revell, L.J., 2012. Phytools: an R package for phylogenetic comparative biology (and other things). Methods Ecol. Evol. 3, 217–223.
Rohlf, F.J., 2015. The tps series of software. Hystrix 26, 9–12.
Ronquist, F., 1997. Dispersal-vicariance analysis: a new approach to the quantification of historical biogeography. Syst. Biol. 46, 195–203.
Ronquist, F. and Huelsenbeck, J.P., 2003. MrBayes 3: Bayesian phylogenetic inference under mixed models. Bioinformatics 19, 1572–1574.
Rouhan, G., Lorence, D.H., Motley, T.J., Hanks, J.G. and Moran, R.C., 2008. Systematic revision of *Elaphoglossum* (Dryopteridaceae) in French Polynesia, with the description of three new species. Bot. J. Linn. 158, 309–331.
Ruhfel, B., Lindsay, S. and Davis, C.C., 2008. Phylogenetic placement of *Rheopteris* and the polyphyly of *Monogramma* (Pteridaceae s.l.): evidence from *rbcL* sequence data. Syst. Bot. 33, 37–43.
Schneider, C.A., Rasband, W.S. and Eliceiri, K.W., 2012. NIH image to ImageJ: 25 years of image analysis. Nat. Methods 9, 671–675.
Schuettpelz, E. and Pryer, K.M., 2009. Evidence for a Cenozoic radiation of ferns in an angiosperm-dominated canopy. PANS 106, 11200–11205.
Schuettpelz, E., Chen, C.-W., Kessler, M., Pinson, J.B., Johnson, G., Davila, A., Cochran, A.T., Huiet, L. and Pryer, K.M., 2016. A revised generic classification of vittarioid ferns (Pteridaceae) based on molecular, micromorphological, and geographic data. Taxon 65, 708–722.
Silvestro, D., Antonelli, A., Scharn, R., Bacon, C.D., Carvalho, F.A., Condamine, F.L. and Zizka, A., 2018. Amazonia is the primary source of Neotropical biodiversity. PNAS 115, 6034–6039.
Simmons, M.P., 2017. Mutually exclusive phylogenomic inferences at the root of the angiosperms: *Amborella* is supported as sister and observed variability is biased. Cladistics 33, 488–512.
Smith, A.C., 1936. Fijian plant studies. Bulletin 141. Bernice P. Bishop Museum, Honolulu.
Sprengel, K., 1827. Systema vegetabilium, 16th edition. Sumtibus Librariae Dieterichianae, Gottingae.
Stamatakis, A., 2014. RAxML version 8: a tool for phylogenetic analysis and post-analysis of large phylogenies. Bioinformatics 30, 1312–1313.
Swofford, D.L., 2002. PAUP*: Phylogenetic analysis using parsimony, version 4.0a. Sinauer, Sunderland, MA.
Taberlet, P., Gielly, L., Pautou, G. and Bouvet, J., 1991. Universal primers for amplification of three noncoding regions of chloroplast DNA. Plant Mol. Biol. 17, 1105–1109.
Taiwan Pteridophyte Group (TPG), 2019. Updating Taiwanese pteridophyte checklist: a new phylogenetic classification. Taiwania 64, 367–395.
Vasconcelos, T.N.C., Proença, C.E.B., Ahmad, B., Aguilar, D.S., Aguilar, R., Amorim, B.S., Campbell, K., Costa, I.R., De-Carvalho, P.S., Faria, J.E.Q., Giaretta, A., Kooij, P.W., Lima, D.F., Mazine, F.F., Peguero, B., Prenner, G., Santos, M.F., Soewarto, J., Wingler, A. and Lucas, E.J., 2017. Myrteae phylogeny, calibration, biogeography and diversification patterns: increased understanding in the most species rich tribe of Myrtaceae. Mol. Phylogenet. Evol. 109, 113–137.
Wickham, W., 2009. ggplot2: elegant graphics for data analysis. Springer-Verlag, New York.
Zhang, X.C., 1998. Genus *Antrophyum* Kaulf. from China and neighboring regions. Bull. Bot. Res. 18, 107–118.

Supporting Information

Additional supporting information may be found online in the Supporting Information section at the end of the article.

Fig. S1. *Antrophyum* phylogeny resulting from maximum likelihood analysis of *chlL* gene.

Fig. S2. *Antrophyum* phylogeny resulting from maximum likelihood analysis of *matK* gene.

Fig. S3. *Antrophyum* phylogeny resulting from maximum likelihood analysis of *ndhF* gene.

Fig. S4. *Antrophyum* phylogeny resulting from maximum likelihood analysis of *trnL-F* region.

Fig. S5. *Antrophyum* phylogeny resulting from Bayesian inference of concatenated alignment.

Fig. S6. *Antrophyum* phylogeny resulting from maximum likelihood analysis of concatenated alignment.

Fig. S7. *Antrophyum* phylogeny resulting from maximum parsimony analysis of concatenated alignment.

Fig. S8. Frond length of 34 *Antrophyum* species.

Fig. S9. Frond width of 34 *Antrophyum* species.

Fig. S10. Frond length/width ratio of 34 *Antrophyum* species.

Fig. S11. Paraphyses length of 34 *Antrophyum* species.

Fig. S12. Paraphyses width of 34 *Antrophyum* species.

Fig. S13. Paraphyses length/width ratio of 34 *Antrophyum* species.

Fig. S14. Scale length of 33 *Antrophyum* species.

Fig. S15. Scale width of 33 *Antrophyum* species.

Fig. S16. Scale cell wall thickness of 33 *Antrophyum* species.

Fig. S17. Original results from ancestral range estimation for *Antrophyum* using BioGeoBEARS.

Fig. S18. Frequency (mean and SD) of dispersal events (range expansion and founder events) across 1000 biogeographical stochastic mapping (BSM) replicates.

Fig. S19. Frequency of biogeographic events over time.

Table S1. Voucher specimens and GenBank accession numbers used in this study.

Table S2. *Post-hoc* Tukey HSD pairwise test of paraphyses length.

Table S3. *Post-hoc* Tukey HSD pairwise test of paraphyses width.

Table S4. *Post-hoc* Tukey HSD pairwise test of rhizome scale cell walls thickness.

Table S5. Names belonging to the *Antrophyum reticulatum* complex.